



Strain gradient solution for a finite-domain Eshelby-type plane strain inclusion problem and Eshelby's tensor for a cylindrical inclusion in a finite elastic matrix

H.M. Ma, X.-L. Gao *

Department of Mechanical Engineering, Texas A&M University, 3123 TAMU, College Station, TX 77843-3123, USA

ARTICLE INFO

Article history:

Received 13 May 2010

Received in revised form 4 August 2010

Available online 16 September 2010

Keywords:

Eshelby tensor

Cylindrical inclusion

Eigenstrain

Size effect

Boundary effect

Strain gradient

Plane strain

ABSTRACT

A solution for the finite-domain Eshelby-type inclusion problem of a finite elastic body containing a plane strain inclusion prescribed with a uniform eigenstrain and a uniform eigenstrain gradient is derived in a general form using a simplified strain gradient elasticity theory (SSGET). The formulation is facilitated by an extended Betti's reciprocal theorem and an extended Somigliana's identity based on the SSGET and suitable for plane strain problems. The disturbed displacement field is obtained in terms of the SSGET-based Green's function for an infinite plane strain elastic body, which differs from that in earlier studies using the three-dimensional Green's function. The solution reduces to that of the infinite-domain inclusion problem when the boundary effect is suppressed. The problem of a cylindrical inclusion embedded concentrically in a finite plane strain cylindrical elastic matrix of an enhanced continuum is analytically solved for the first time by applying the general solution, with the Eshelby tensor and its average over the circular cross section of the inclusion obtained in closed forms. This Eshelby tensor, being dependent on the position, inclusion size, matrix size, and a material length scale parameter, captures the inclusion size and boundary effects, unlike existing ones. It reduces to the classical elasticity-based Eshelby tensor for the cylindrical inclusion in an infinite matrix if both the strain gradient and boundary effects are not considered. Numerical results quantitatively show that the inclusion size effect can be quite large when the inclusion is very small and that the boundary effect can dominate when the inclusion volume fraction is very high. However, the inclusion size effect is diminishing with the increase of the inclusion size, and the boundary effect is vanishing as the inclusion volume fraction becomes sufficiently low.

© 2010 Elsevier Ltd. All rights reserved.

1. Introduction

Eshelby's eigenstrain method and fourth-order strain transformation tensor (Eshelby, 1957, 1959) play a key role in homogenization methods for heterogeneous materials (e.g., Hill, 1965; Budiansky, 1965; Mori and Tanaka, 1973; Weng, 1990; Huang et al., 1994; Le Quang and He, 2007; Genin and Birman, 2009). However, the Eshelby tensor in its original form (Eshelby, 1957, 1959) is based on *classical elasticity* and cannot account for the particle (inclusion) size effect experimentally observed in some composites filled with micro- and nano-particles (e.g., Vollenberg and Heikens, 1989; Reynaud et al., 2001; Cho et al., 2006). Moreover, this classical Eshelby tensor is for an inclusion embedded in an *infinite* elastic matrix and is unable to incorporate the effect of finite boundaries. As a result, the homogenization methods employing the classical elasticity-based Eshelby tensor cannot capture the particle size and boundary effects. Hence, there has been a need to obtain Eshelby's tensor for an inclusion in a *finite* matrix using

higher-order (non-classical) elasticity theories, which, unlike classical elasticity, contain material length scale parameters and are capable of explaining microstructure-dependent size (and other) effects.

For the Eshelby-type inclusion problem of an *infinite* homogeneous isotropic elastic body containing an inclusion, a number of studies have been conducted using various higher-order elasticity theories, which include a micropolar theory (Cheng and He, 1995, 1997; Ma and Hu, 2006), a microstretch theory (Liu and Hu, 2004; Kiris and Inan, 2006; Ma and Hu, 2007), a modified couple stress theory (Zheng and Zhao, 2004), a strain gradient theory (Zhang and Sharma, 2005), and a simplified strain gradient theory (Gao and Ma, 2009, 2010a,b; Ma and Gao, 2010a). These studies have led to analytical solutions of the inclusion problem and resulted in closed-form expressions of the Eshelby tensor for a spherical or cylindrical inclusion in an infinite elastic body based on higher-order elasticity theories.

On the other hand, for the problem of an inclusion embedded in a *finite* homogeneous isotropic elastic matrix, only a few analytical studies have been performed even in the context of *classical elasticity*. The first one was provided by Kinoshita and Mura (1984). They

* Corresponding author. Tel.: +1 979 845 4835; fax: +1 979 845 3081.

E-mail address: xlga@tamu.edu (X.-L. Gao).

proved the existence and uniqueness of a second-order Neumann tensor, which reduces to the Green's function (also a second-order tensor) when the body is unbounded. The use of the Neumann tensor would give the solution of an inclusion problem in a bounded elastic body. However, the determination of this Neumann tensor for a bounded elastic body is rather challenging, and only the Neumann tensor for a half space was provided in Kinoshita and Mura (1984). More recently, Li et al. (2005, 2007) analytically obtained the Eshelby's tensors for a two-dimensional (2-D) finite-domain circular inclusion problem and a three-dimensional (3-D) finite-domain spherical inclusion problem using Somigliana's identity and Green's functions in classical elasticity.

The first study on *finite-domain* inclusion problems based on a *higher-order* elasticity theory has recently been reported by Gao and Ma (2010a), where a simplified strain gradient elasticity theory (SSGET) (e.g., Gao and Park, 2007) is used and the problem of a spherical inclusion embedded concentrically in a finite spherical elastic body is analytically solved. The solution of this finite-domain inclusion problem is obtained using the SSGET-based 3-D Green's function derived in Gao and Ma (2009) and includes the solution for its counterpart infinite-domain inclusion problem published earlier as a limiting case.

The current study aims to provide the solution for the finite-domain Eshelby-type inclusion problem of a finite homogeneous isotropic elastic body containing a plane strain inclusion prescribed with a uniform eigenstrain and a uniform eigenstrain gradient using the SSGET. The present solution utilizes the SSGET-based Green's function for a plane strain elastic body, which differs from the 3-D Green's function used in Gao and Ma (2010a) for the finite-domain spherical inclusion problem and in Ma and Gao (2010a) for the infinite-domain plane strain and cylindrical inclusion problems.

The rest of the paper is organized as follows. In Section 2, the SSGET is first reviewed, which is followed by the derivation of a general solution for the finite-domain Eshelby-type plane strain inclusion problem using an extended Betti's reciprocal theorem and an extended Somigliana's identity based on the SSGET and suitable for plane strain problems. The finite-domain cylindrical inclusion problem is solved in Section 3 by applying the general formulas derived in Section 2, which leads to closed-form expressions of the Eshelby tensor and its area average. In Section 4, sample numerical results are presented to quantitatively show the dependence of the components of the Eshelby tensor and its average obtained in Section 3 on the position, inclusion size, and inclusion volume fraction, where the size and boundary effects are observed and discussed. The paper concludes in Section 5 with a summary and some remarks.

2. Solution for a plane strain inclusion in a finite domain

2.1. Simplified strain gradient elasticity theory (SSGET)

The SSGET is the simplest strain gradient elasticity theory evolving from Mindlin's pioneering work (Mindlin, 1964, 1965; Mindlin and Eshel, 1968). It is also known as the first gradient elasticity theory of Helmholtz type and the dipolar gradient elasticity theory (Gao and Ma, 2010a). According to this theory, the strain energy density function, w , for an isotropic linearly elastic material has the form (e.g., Gao and Park, 2007; Gao and Ma, 2010b):

$$w = w(\varepsilon_{ij}, \kappa_{ijk}) = \frac{1}{2} \lambda \varepsilon_{ii} \varepsilon_{jj} + \mu \varepsilon_{ij} \varepsilon_{ij} + L^2 \left(\frac{1}{2} \lambda \kappa_{iik} \kappa_{jjk} + \mu \kappa_{ijk} \kappa_{ijk} \right), \quad (1)$$

where λ and μ are the Lamé constants in classical elasticity, L is a material length scale parameter, and ε_{ij} and κ_{ijk} are, respectively, the components of the infinitesimal strain, $\boldsymbol{\varepsilon} = \varepsilon_{ij} \mathbf{e}_i \otimes \mathbf{e}_j$, and the strain gradient, $\boldsymbol{\kappa} \equiv \nabla \boldsymbol{\varepsilon} = \kappa_{ijk} \mathbf{e}_i \otimes \mathbf{e}_j \otimes \mathbf{e}_k$, given by

$$\varepsilon_{ij} = \frac{1}{2} (u_{i,j} + u_{j,i}), \quad \kappa_{ijk} \equiv \varepsilon_{ij,k} = \frac{1}{2} (u_{ijk} + u_{jik}), \quad (2a, b)$$

with u_i being the components of the displacement vector $\mathbf{u} = u_i \mathbf{e}_i$.

The constitutive equations are obtained from Eq. (1) as

$$\tau_{ij} = \frac{\partial w}{\partial \varepsilon_{ij}} = \lambda \varepsilon_{ll} \delta_{ij} + 2\mu \varepsilon_{ij} = C_{ijkl} \varepsilon_{kl} = \tau_{ji}, \quad (3)$$

$$\mu_{ijk} = \frac{\partial w}{\partial \kappa_{ijk}} = L^2 (\lambda \varepsilon_{ll} \delta_{ij} + 2\mu \varepsilon_{ij})_{,k} = L^2 C_{ijmn} \kappa_{mnk} = L^2 \tau_{ij,k} = \mu_{jik}, \quad (4)$$

where τ_{ij} are the components of the Cauchy stress, $\boldsymbol{\tau} = \tau_{ij} \mathbf{e}_i \otimes \mathbf{e}_j$, μ_{ijk} are the components of the double stress, $\boldsymbol{\mu} = \mu_{ijk} \mathbf{e}_i \otimes \mathbf{e}_j \otimes \mathbf{e}_k$, δ_{ij} is the Kronecker delta, and C_{ijkl} are the components of the elastic stiffness tensor for isotropic elastic materials given by $C_{ijkl} = \lambda \delta_{ij} \delta_{kl} + \mu (\delta_{ik} \delta_{jl} + \delta_{il} \delta_{jk})$.

The equilibrium equations are

$$\sigma_{ij,j} + f_i = 0, \quad (5)$$

where f_i are the components of the body force, and σ_{ij} are the components of the total stress, $\boldsymbol{\sigma} = \sigma_{ij} \mathbf{e}_i \otimes \mathbf{e}_j$, which are related to the Cauchy stress components τ_{ij} through

$$\sigma_{ij} \equiv \tau_{ij} - \mu_{ijk,k} = \tau_{ij} - L^2 \tau_{ij,kk}. \quad (6)$$

Using Eqs. (2a,b)–(4) and (6) in Eq. (5) leads to the Navier-like displacement-equations of equilibrium as

$$(\lambda + \mu) u_{i,jj} + \mu u_{j,kk} - L^2 [(\lambda + \mu) u_{i,jj} + \mu u_{j,kk}]_{,mm} + f_j = 0 \quad \text{in } \Omega, \quad (7)$$

where Ω is the region occupied by the elastic material.

The complete boundary conditions, determined simultaneously with the equilibrium equations listed in Eq. (5) using a variational formulation (Gao and Park, 2007), have the form:

$$\left. \begin{aligned} t_i &= \bar{t}_i \quad \text{or} \quad u_i = \bar{u}_i, \\ q_i &= \bar{q}_i \quad \text{or} \quad u_{i,l} n_l = \frac{\partial \bar{u}_i}{\partial n} \end{aligned} \right\} \quad \text{on } \partial\Omega, \quad (8a, b)$$

with

$$t_i = \sigma_{ij} n_j - \left(\mu_{ijk} n_k \right)_j + \left(\mu_{ijk} n_k n_l \right)_j n_j, \quad q_i = \mu_{ijk} n_j n_k, \quad (8c, d)$$

where t_i and q_i are, respectively, the components of the Cauchy traction vector and double stress traction vector, $\partial\Omega$ is the smooth bounding surface of Ω , and n_i is the outward unit normal vector on $\partial\Omega$. In Eqs. (8a,b), the overbar represents the prescribed value. Note that the standard index notation, together with the Einstein summation convention, is used in Eqs. (1)–(8a–d) and throughout this paper, with each Latin index (subscript) ranging from 1 to 3 and each Greek index ranging from 1 to 2, unless otherwise stated.

Eqs. (7) and (8a,b), along with Eqs. (2a,b)–(4) and (6), define the boundary value problem in terms of displacement in the SSGET. Clearly, the material length scale parameter L is explicitly involved in Eq. (7) in addition to the two Lamé constants λ and μ . When the strain gradient effect is absent (i.e., $L = 0$), it follows from Eq. (4) that $\mu_{ijk} = 0$ and from Eq. (6) that $\sigma_{ij} = \tau_{ij}$. As a result, Eqs. (7) and (8a,b) reduce to the governing equations and the boundary conditions in terms of displacement in classical elasticity (e.g., Timoshenko and Goodier, 1970; Gao and Rowlands, 2000).

For an infinite elastic body loaded by a unit concentrated force, Eq. (7), subject to the boundary conditions of \mathbf{u} and its first-, second- and third-order spatial derivatives vanishing at infinity, has been solved in Gao and Ma (2009) by using Fourier transforms to obtain the SSGET-based 3-D Green's function expressed in terms of elementary functions. This Green's function has been subsequently used to solve several inclusion problems involving an infinite or a finite 3-D elastic body containing an inclusion (Gao and Ma, 2009, 2010a,b; Ma and Gao, 2010a).

For a plane strain problem in the x_1x_2 -plane, the 2-D Green's function based on the SSGET has been obtained by Polyzos et al. (2003) as

$$G_{\alpha\beta}(\mathbf{r}) = \frac{1}{8\pi\mu(1-\nu)} \left[\Psi(r)\delta_{\alpha\beta} - X(r)r_\alpha^0 r_\beta^0 \right], \quad (9)$$

with

$$\begin{aligned} \Psi(r) &= -(3-4\nu)\ln r + \frac{2L^2}{r^2} - (3-4\nu)K_0\left(\frac{r}{L}\right) \\ &\quad - K_2\left(\frac{r}{L}\right), \quad X(r) \\ &= -1 + \frac{4L^2}{r^2} - 2K_2\left(\frac{r}{L}\right), \end{aligned} \quad (10a, b)$$

where ν is the Poisson's ratio, r is the magnitude of $\mathbf{r} = \mathbf{p} - \mathbf{z}$ (with $r = \sqrt{(p_1 - z_1)^2 + (p_2 - z_2)^2}$), \mathbf{z} is the point where the concentrated force is applied, \mathbf{p} is the point of interest, $r_\alpha^0 = r_\alpha/r$ are the components of the unit vector $\mathbf{r}^0 = \mathbf{r}/r$, and $K_n(\cdot)$ ($n = 0, 2$) is the modified Bessel function of the second kind of the n th order, which satisfies the following asymptotic relation (e.g., Arfken and Weber, 2005):

$$K_n(z) \sim \sqrt{\frac{\pi}{2z}} e^{-z} \quad \text{as } z \rightarrow \infty. \quad (10c)$$

When the strain gradient effect is not considered (i.e., when $L = 0$), Eqs. (9) and (10a,b) reduce to

$$G_{\alpha\beta}^c(\mathbf{r}) = \frac{1}{8\pi\mu(1-\nu)} \left[-(3-4\nu)(\ln r)\delta_{\alpha\beta} + r_\alpha^0 r_\beta^0 \right], \quad (11)$$

which is the 2-D Green's function for the plane strain case in classical elasticity (e.g., Paris and Canas, 1997). In reaching Eq. (11), use has been made of the results: $K_0(r/L) = 0$, $K_2(r/L) = 0$ as $L \rightarrow 0$, which follow from Eq. (10c) directly.

To facilitate the differentiation of the Green's function involved in determining the Eshelby's tensor in the next section, the 2-D Green's function $G_{\alpha\beta}(\mathbf{r}) = G_{\beta\alpha}(\mathbf{r})$ given in Eqs. (9) and (10a,b) can be rewritten as

$$G_{\alpha\beta}(\mathbf{r}) = A(r)\delta_{\alpha\beta} + \frac{\partial^2 B(r)}{\partial r_\alpha \partial r_\beta}, \quad (12)$$

where

$$\begin{aligned} A(r) &= -\frac{1}{2\pi\mu} \left[\ln r + K_0\left(\frac{r}{L}\right) \right], \quad B(r) \\ &= \frac{1}{16\pi\mu(1-\nu)} \left[r^2 \ln r - \frac{r^2}{2} + 4L^2 \ln r + 4L^2 K_0\left(\frac{r}{L}\right) \right]. \end{aligned} \quad (13a, b)$$

Note that in reaching Eqs. (12) and (13a,b) use has been made of the following relation:

$$\frac{\partial^2 f(r)}{\partial r_\alpha \partial r_\beta} = \left(\frac{d^2 f}{dr^2} - \frac{1}{r} \frac{df}{dr} \right) r_\alpha^0 r_\beta^0 + \left(\frac{1}{r} \frac{df}{dr} \right) \delta_{\alpha\beta}, \quad (14)$$

where $f(r)$ is an arbitrary scalar-valued function of r .

The 2-D Green's function listed in Eq. (12) gives the displacement in an infinite plane strain elastic body Ω_∞ induced by a unit concentrated body force, $f_\alpha(\mathbf{y}) = \delta(\mathbf{y} - \mathbf{x})e_\alpha(\mathbf{x})$, in the x_1x_2 -plane (see Fig. 1) through

$$u_\alpha(\mathbf{y}) = G_{\alpha\beta}(\mathbf{y} - \mathbf{x})e_\beta(\mathbf{x}), \quad (15)$$

where \mathbf{y} is a point of interest in Ω_∞ , \mathbf{x} is the point where the concentrated body force is applied, and $e_\beta(\mathbf{x})$ is the β th component of the unit force. Once the displacement field becomes known, the strain and stress fields will be readily determined from Eqs. (2a,b)–(4).

For a finite region R in the x_1x_2 -plane that is cut out of the infinite region Ω_∞ (see Fig. 1(b)), the Cauchy stress traction, t_α , and the double stress traction, q_α , on the boundary of the region R , ∂R , can be obtained as

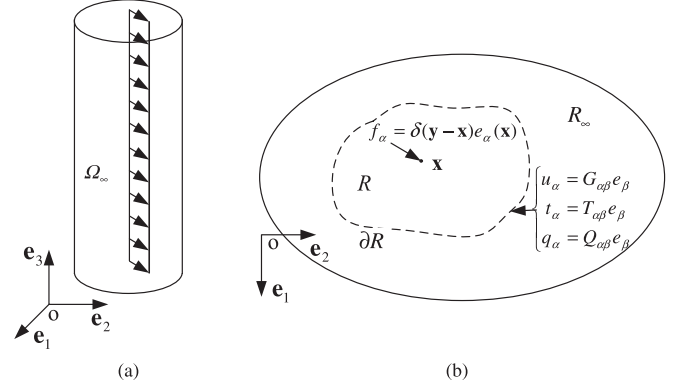


Fig. 1. An infinite plane strain elastic body (a) and its cross section (b).

$$t_\alpha(\mathbf{y}) = T_{\alpha\beta}(\mathbf{y} - \mathbf{x})e_\beta(\mathbf{x}), \quad q_\alpha(\mathbf{y}) = Q_{\alpha\beta}(\mathbf{y} - \mathbf{x})e_\beta(\mathbf{x}), \quad (16a, b)$$

where $T_{\alpha\beta}(\mathbf{y} - \mathbf{x})$ and $Q_{\alpha\beta}(\mathbf{y} - \mathbf{x})$ are, respectively, the second-order Cauchy traction and double stress traction transformation tensors related to the Green's function $G_{\alpha\beta}(\mathbf{y} - \mathbf{x})$ by (see Appendix A for derivations)

$$\begin{aligned} T_{\alpha\gamma} &= P_{\alpha\beta\gamma}n_\beta - L^2(\nabla^2 P_{\alpha\beta\gamma})n_\beta - L^2P_{\alpha\beta\gamma,0\beta}n_0 + L^2P_{\alpha\beta\gamma,0\gamma}n_0n_\gamma n_\beta \\ &\quad + L^2P_{\alpha\beta\gamma,0}(-n_{0,\beta} + n_{0,\gamma}n_\gamma n_\beta + n_{0,\gamma}n_\gamma n_\beta), \end{aligned} \quad (17a)$$

$$Q_{\alpha\gamma} = L^2P_{\alpha\beta\gamma,\gamma}n_\beta n_\gamma, \quad (17b)$$

where

$$P_{\alpha\beta\gamma} \equiv \lambda G_{0\gamma,0}\delta_{\alpha\beta} + \mu(G_{\alpha\gamma,\beta} + G_{\beta\gamma,\alpha}). \quad (17c)$$

When $L = 0$, Eqs. (17a,b) reduce to

$$\begin{aligned} T_{\alpha\gamma}^c &= -\frac{1}{4\pi(1-\nu)r} \left\{ [(1-2\nu)\delta_{\alpha\gamma} + 2r_\alpha^0 r_\gamma^0] r_\beta^0 n_\beta + (1-2\nu)(r_\alpha^0 n_\gamma - r_\gamma^0 n_\alpha) \right\}, \\ Q_{\alpha\gamma}^c &= 0, \end{aligned} \quad (18a, b)$$

which are the traction transformation tensors based on classical elasticity. It can be readily shown that Eq. (18a) is the same as that provided in Paris and Canas (1997) for the plane strain case (see their Eq. (5.4.25)).

2.2. Inclusion problem solution

Consider a plane strain problem where a prismatic inclusion, Ω_I , with a cross section of arbitrary shape, R_I , and an infinite length is embedded in a homogeneous isotropic elastic body, Ω , with a finite cross section of arbitrary shape, R , and an infinite length (see Fig. 2).

A uniform eigenstrain $\boldsymbol{\varepsilon}^*$ and a uniform eigenstrain gradient $\boldsymbol{\kappa}^*$ are prescribed inside Ω_I and vanish outside Ω_I . For the current plane strain problem, only the components of $\boldsymbol{\varepsilon}^*$ and $\boldsymbol{\kappa}^*$ in the x_1x_2 -plane are non-vanishing and independent of x_3 . That is,

$$\varepsilon_{\alpha\beta}^* \neq 0, \quad \varepsilon_{3i}^* = 0, \quad \kappa_{\alpha\beta\gamma}^* \neq 0, \quad \kappa_{\alpha\beta 3}^* = \kappa_{3ij}^* = 0. \quad (19)$$

Note that $\boldsymbol{\varepsilon}^*$ and $\boldsymbol{\kappa}^*$ may have been induced by inelastic deformations such as thermal expansion, phase transformation, residual stress, and plastic flow (e.g., Qu and Cherkaoui, 2006; Li and Wang, 2008; Gao and Ma, 2009). Also, $\boldsymbol{\kappa}^*$ can be prescribed independently of $\boldsymbol{\varepsilon}^*$ (Ma and Gao, 2010a). Besides $\boldsymbol{\varepsilon}^*$ and $\boldsymbol{\kappa}^*$, there is no body force or surface force acting in the elastic body containing the inclusion. Hence, the displacement, strain and stress fields induced by the presence of $\boldsymbol{\varepsilon}^*$ and $\boldsymbol{\kappa}^*$ here are disturbed fields, which may be superposed to those caused by applied body and/or surface forces.

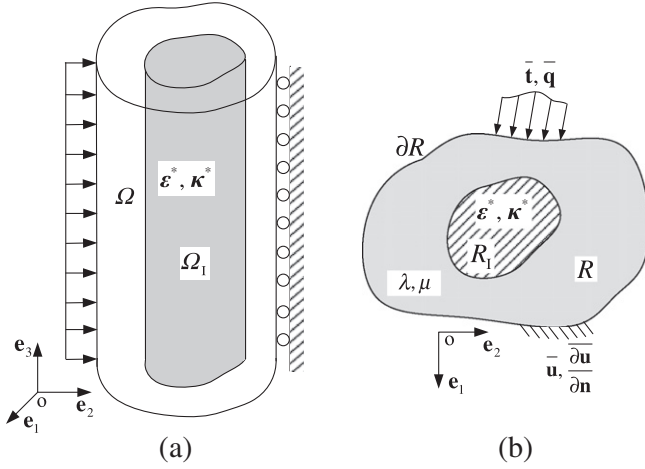


Fig. 2. Inclusion in a finite plane strain body (a) with an arbitrary cross section (b).

As shown in Gao and Ma (2010a), the displacement field due to the eigenstrain ε^* and eigenstrain gradient κ^* (see Eq. (19)) can be obtained from solving the equilibrium equations involving the body force:

$$f_x = -C_{\alpha\beta\gamma\theta}(\varepsilon_{\gamma\theta,\beta}^* - L^2\kappa_{\gamma\theta\chi,\chi\beta}^*), \quad (20)$$

where $C_{\alpha\beta\gamma\theta}$ is the elastic stiffness tensor for isotropic elastic materials given by

$$C_{\alpha\beta\gamma\theta} = \lambda\delta_{\alpha\beta}\delta_{\gamma\theta} + \mu(\delta_{\alpha\gamma}\delta_{\beta\theta} + \delta_{\alpha\theta}\delta_{\beta\gamma}). \quad (21)$$

To solve the finite-domain inclusion problem satisfying Eqs. (7), (8a,b), (19) and (20), the extended Betti's reciprocal theorem based on the SSGT (Gao and Ma, 2010a) will be used. For plane strain deformations, this theorem can be expressed as

$$\begin{aligned} \int_R f_x^{(I)} u_x^{(II)} dA + \int_{\partial R} [t_x^{(I)} u_x^{(II)} + q_x^{(I)} u_{x,\beta}^{(II)} n_\beta] dS \\ = \int_R f_x^{(II)} u_x^{(I)} dA + \int_{\partial R} [t_x^{(II)} u_x^{(I)} + q_x^{(II)} u_{x,\beta}^{(I)} n_\beta] dS, \end{aligned} \quad (22)$$

where the superscripts “(I)” and “(II)” represent two loading sets, R is the cross-sectional area in the x_1x_2 -plane, ∂R is the boundary curve of R , $\mathbf{n} = n_\alpha \mathbf{e}_\alpha$ is the outward unit normal vector on ∂R , f_x is the component of the body force, t_x and q_x are, respectively, the components of the Cauchy traction and double stress traction defined in Eqs. (8c,d), and dA and dS are, respectively, the differential area and line elements.

The loading by ε^* and κ^* in the current inclusion problem shown Fig. 2 is taken to be the loading set (II), while that by a unit concentrated body force applied at a point inside a finite elastic body identical to that of Ω (see Figs. 1(b) and 2(a)) as the loading set (I). For the latter, the finite elastic body is cut out of an infinite body Ω_∞ having the same elastic properties, and the displacement, Cauchy traction and double stress traction at any point $\mathbf{y} \in \partial\Omega$ (the cutting surface) are given by Eqs. (15), (16a) and (16b), respectively. Using Eq. (20) for the set (II) and Eqs. (15) and (16a,b) and $f_x^{(I)}(\mathbf{y}) = \delta(\mathbf{y} - \mathbf{x})e_x(\mathbf{x})$ for the set (I) in Eq. (22) leads to

$$\begin{aligned} u_\beta(\mathbf{x}) = \int_R C_{\alpha\phi\gamma\theta} [\varepsilon_{\gamma\theta,\phi}^* G_{\alpha\beta,\phi}(\mathbf{y} - \mathbf{x}) + L^2 \kappa_{\gamma\theta\chi}^* G_{\alpha\beta,\chi\phi}(\mathbf{y} - \mathbf{x})] dA_y \\ - \int_{\partial R} [T_{\alpha\beta}(\mathbf{y} - \mathbf{x}) u_\alpha + Q_{\alpha\beta}(\mathbf{y} - \mathbf{x}) u_{\alpha,\gamma} n_\gamma] dS_y \\ + \int_{\partial R} [G_{\alpha\beta}(\mathbf{y} - \mathbf{x}) t_\alpha + G_{\alpha\beta,\gamma}(\mathbf{y} - \mathbf{x}) q_\alpha n_\gamma] dS_y, \end{aligned} \quad (23)$$

where the derivatives are with respect to \mathbf{y} (the integration variable), and use has been made of the fact that the eigenstrain and

eigenstrain gradient vanish on the boundary of the finite body $\partial\Omega$ (and thus on ∂R , the projection of $\partial\Omega$ on the x_1x_2 -plane), which is outside the inclusion. Note that in Eq. (23) and in the sequel, the superscript “(II)” has been dropped for convenience, since the displacement, traction and double stress traction involved in Eq. (23) and subsequent equations are all for the inclusion problem under the loading set (II) shown in Fig. 2. It is seen from Eq. (23) that the displacement contains contributions from field quantities distributed both in R and on its boundary ∂R . If the two line integrals in Eq. (23) are suppressed, the disturbed displacement field in Eq. (23) reduces to that for the problem of an inclusion in an infinite elastic body based on the SSGT (Ma and Gao, 2010a), where no boundary effect is considered. That is, the two line integrals in Eq. (23) represent the boundary effect due to the finite size of the elastic body and/or the constraints existing on the finite boundary. Eq. (23) can be viewed as an extended Somigliana's identity based on the SSGT for the plane strain inclusion problem under consideration.

If the microstructure-dependent strain gradient effect is neglected by setting $L = 0$, the higher-order terms involved in Eq. (23) vanish (with $\mu_{\alpha\beta\gamma} = 0$, $q_\alpha = 0$ and $Q_{\alpha\beta} = 0$ from Eqs. (4), (8d) and (17b), respectively), and Eq. (23) reduces to

$$\begin{aligned} u_\beta(\mathbf{x}) = \int_R C_{\alpha\phi\gamma\theta} \varepsilon_{\gamma\theta,\phi}^* G_{\alpha\beta,\phi}(\mathbf{y} - \mathbf{x}) dA_y \\ + \int_{\partial R} [-T_{\alpha\beta}^C(\mathbf{y} - \mathbf{x}) u_\alpha + G_{\alpha\beta}^C(\mathbf{y} - \mathbf{x}) t_\alpha] dS_y, \end{aligned} \quad (24)$$

where $G_{\alpha\beta}^C$ is the Green's function for an infinite plane strain elastic body in classical elasticity listed in Eq. (11), $G_{\alpha\beta,\phi}^C \equiv \partial G_{\alpha\beta}^C(\mathbf{y} - \mathbf{x}) / \partial y_\phi$, $T_{\alpha\beta}^C$ is the classical Cauchy traction transformation tensor given in Eq. (18a), and t_α is the traction related to the Cauchy stress $\tau_{\alpha\beta}$ by $t_\alpha = \tau_{\alpha\beta} n_\beta$. It can be readily verified that Eq. (24) is the same as the Somigliana's identity in classical elasticity for the plane strain inclusion problem used in Li et al. (2005).

For the homogeneous Dirichlet-like boundary conditions of $u_\alpha = 0$ and $u_{\alpha,\gamma} n_\gamma = 0$ on ∂R , Eq. (23) gives

$$\begin{aligned} u_\beta(\mathbf{x}) = \int_R C_{\alpha\phi\gamma\theta} [\varepsilon_{\gamma\theta,\phi}^* G_{\alpha\beta,\phi}(\mathbf{y} - \mathbf{x}) + L^2 \kappa_{\gamma\theta\chi}^* G_{\alpha\beta,\chi\phi}(\mathbf{y} - \mathbf{x})] dA_y \\ + \int_{\partial R} [G_{\alpha\beta}(\mathbf{y} - \mathbf{x}) t_\alpha + G_{\alpha\beta,\gamma}(\mathbf{y} - \mathbf{x}) q_\alpha n_\gamma] dS_y, \end{aligned} \quad (25)$$

which is the disturbed displacement field in the finite plane strain elastic body induced by the eigenstrain ε^* and eigenstrain gradient κ^* . In Eq. (25), t_α and q_α on ∂R can be obtained from u_β using Eqs. (2a,b)–(4), (6) and (8c,d).

Similarly, for the homogeneous Neumann-like boundary conditions of $t_\alpha = 0$ and $q_\alpha = 0$ on ∂R , Eq. (23) yields

$$\begin{aligned} u_\beta(\mathbf{x}) = \int_R C_{\alpha\phi\gamma\theta} [\varepsilon_{\gamma\theta,\phi}^* G_{\alpha\beta,\phi}(\mathbf{y} - \mathbf{x}) + L^2 \kappa_{\gamma\theta\chi}^* G_{\alpha\beta,\chi\phi}(\mathbf{y} - \mathbf{x})] dA_y \\ - \int_{\partial R} [T_{\alpha\beta}(\mathbf{y} - \mathbf{x}) u_\alpha + Q_{\alpha\beta}(\mathbf{y} - \mathbf{x}) u_{\alpha,\gamma} n_\gamma] dS_y \end{aligned} \quad (26)$$

as the disturbed displacement field in the finite plane strain elastic body induced by ε^* and κ^* .

Clearly, Eqs. (25) and (26) are integral equations where the unknown displacement components u_β appear both inside and outside the line integral in each equation. It is very challenging to obtain analytical solutions of such integral equations even for inclusion problems involving simple-shape elastic bodies and inclusions. Hence, only the inclusion problems obeying Eq. (25), which are associated with the simpler homogeneous Dirichlet-like boundary conditions, will continue to be formulated in the rest of this section.

As stated earlier, the derivatives involved in the integrals in Eqs. (23)–(26) are with respect to the integration variable \mathbf{y} . Note that

$$\frac{\partial G_{\alpha\beta}(\mathbf{y} - \mathbf{x})}{\partial y_\gamma} = -\frac{\partial G_{\alpha\beta}(\mathbf{y} - \mathbf{x})}{\partial x_\gamma}. \quad (27)$$

Using Eq. (27) in Eq. (25) then gives

$$\begin{aligned} u_\beta(\mathbf{x}) = & \int_R C_{\alpha\phi\gamma\theta} \left[-\varepsilon_{\gamma\theta}^* G_{\alpha\beta,\phi}(\mathbf{y} - \mathbf{x}) + L^2 \kappa_{\gamma\theta\chi}^* G_{\alpha\beta,\chi\phi}(\mathbf{y} - \mathbf{x}) \right] dA_y \\ & + \int_{\partial R} [G_{\alpha\beta}(\mathbf{y} - \mathbf{x}) t_\alpha - G_{\alpha\beta,\gamma}(\mathbf{y} - \mathbf{x}) q_\alpha n_\gamma] dS_y. \end{aligned} \quad (28)$$

In Eq. (28) and all of the ensuing equations, the derivatives are taken with respect to \mathbf{x} unless otherwise stated.

Substituting Eq. (28) into Eq. (2a) yields the disturbed strain as

$$\begin{aligned} \varepsilon_{\beta\kappa}(\mathbf{x}) = & \frac{1}{2} \int_R C_{\alpha\phi\gamma\theta} \left[-\varepsilon_{\gamma\theta}^* (G_{\alpha\beta,\phi\kappa} + G_{\alpha\kappa,\phi\beta}) + L^2 \kappa_{\gamma\theta\chi}^* (G_{\alpha\beta,\chi\phi\kappa} + G_{\alpha\kappa,\chi\phi\beta}) \right] dA_y \\ & + \frac{1}{2} \int_{\partial R} [(G_{\alpha\beta,\kappa} + G_{\alpha\kappa,\beta}) t_\alpha - (G_{\alpha\beta,\gamma\kappa} + G_{\alpha\kappa,\gamma\beta}) q_\alpha n_\gamma] dS_y, \end{aligned} \quad (29)$$

where the line integral term represents the boundary effect on the disturbed strain field for the finite-domain inclusion problem.

For uniform ε^* and κ^* inside the inclusion (i.e., $\mathbf{x} \in R_I$), the area integral term in Eq. (29) is identical to the disturbed strain field in an infinite elastic body containing a plane strain inclusion of arbitrary shape derived in Ma and Gao (2010a), which can be written as

$$\varepsilon_{\beta\kappa}^\infty(\mathbf{x}) = S_{\beta\kappa\gamma\theta}^\infty(\mathbf{x}) \varepsilon_{\gamma\theta}^* + T_{\beta\kappa\gamma\theta\chi}^\infty(\mathbf{x}) \kappa_{\gamma\theta\chi}^*, \quad (30a)$$

with

$$S_{\beta\kappa\gamma\theta}^\infty(\mathbf{x}) \equiv -\frac{1}{2} \int_{R_I} C_{\alpha\phi\gamma\theta} (G_{\alpha\beta,\phi\kappa} + G_{\alpha\kappa,\phi\beta}) dA_y, \quad (30b)$$

$$T_{\beta\kappa\gamma\theta\chi}^\infty(\mathbf{x}) \equiv \frac{L^2}{2} \int_{R_I} C_{\alpha\phi\gamma\theta} (G_{\alpha\beta,\chi\phi\kappa} + G_{\alpha\kappa,\chi\phi\beta}) dA_y, \quad (30c)$$

where $S_{\beta\kappa\gamma\theta}^\infty$ and $T_{\beta\kappa\gamma\theta\chi}^\infty$, as defined, are, respectively, the fourth-order Eshelby tensor and the fifth-order Eshelby-like tensor for the plane strain infinite-domain inclusion problem, and the superscript “ ∞ ” can be either “ I ”, representing the *interior* case with \mathbf{x} located inside the inclusion, or “ E ”, representing the *exterior* case with \mathbf{x} located outside the inclusion.

Based on the similarity between the unbounded and bounded cases and Eqs. (30a)–(30c), it is postulated that for the present bounded-domain inclusion problem the disturbed strain field has the form:

$$\varepsilon_{\beta\kappa}(\mathbf{x}) = S_{\beta\kappa\gamma\theta}^F(\mathbf{x}) \varepsilon_{\gamma\theta}^* + T_{\beta\kappa\gamma\theta\chi}^F(\mathbf{x}) \kappa_{\gamma\theta\chi}^*, \quad (31)$$

which is similar to that given in Eqs. (30a) for the unbounded-domain inclusion problem. In Eq. (31), $S_{\beta\kappa\gamma\theta}^F(\mathbf{x})$ and $T_{\beta\kappa\gamma\theta\chi}^F(\mathbf{x})$ denote, respectively, the Eshelby tensor and the Eshelby-like tensor for the current finite-domain inclusion problem.

Using Eqs. (3), (4), (6) and (31) in Eqs. (8c,d) yields

$$t_\alpha = g_{\alpha\gamma\theta} \varepsilon_{\gamma\theta}^* + p_{\alpha\gamma\theta\theta} \kappa_{\gamma\theta\theta}^*, \quad q_\alpha = h_{\alpha\gamma\theta} \varepsilon_{\gamma\theta}^* + d_{\alpha\gamma\theta\theta} \kappa_{\gamma\theta\theta}^*, \quad (32a, b)$$

where

$$g_{\alpha\gamma\theta} \equiv C_{\alpha\beta\kappa\chi} \left[(1 - L^2 \nabla^2) S_{\kappa\chi\gamma\theta}^F n_\beta - (L^2 S_{\kappa\chi\gamma\theta,\phi}^F n_\phi)_\beta + (L^2 S_{\kappa\chi\gamma\theta,\phi}^F n_\phi n_\eta)_\eta n_\beta \right], \quad (33a)$$

$$p_{\alpha\gamma\theta\theta} \equiv C_{\alpha\beta\kappa\chi} \left[(1 - L^2 \nabla^2) T_{\kappa\chi\gamma\theta\theta}^F n_\beta - (L^2 T_{\kappa\chi\gamma\theta\theta,\phi}^F n_\phi)_\beta + (L^2 T_{\kappa\chi\gamma\theta\theta,\phi}^F n_\phi n_\eta)_\eta n_\beta \right], \quad (33b)$$

$$h_{\alpha\gamma\theta} \equiv L^2 C_{\alpha\beta\kappa\chi} S_{\kappa\chi\gamma\theta,\phi}^F n_\beta n_\phi, \quad (33c)$$

$$d_{\alpha\gamma\theta\theta} \equiv L^2 C_{\alpha\beta\kappa\chi} T_{\kappa\chi\gamma\theta\theta,\phi}^F n_\beta n_\phi. \quad (33d)$$

Substituting Eqs. (30a), (31) and (32a,b) into Eq. (29) then yields

$$\begin{aligned} S_{\beta\kappa\gamma\theta}^F \varepsilon_{\gamma\theta}^* + T_{\beta\kappa\gamma\theta\chi}^F \kappa_{\gamma\theta\chi}^* = & S_{\beta\kappa\gamma\theta}^\infty \varepsilon_{\gamma\theta}^* + T_{\beta\kappa\gamma\theta\chi}^\infty \kappa_{\gamma\theta\chi}^* \\ & + \frac{1}{2} \int_{\partial R} \left[(g_{\alpha\gamma\theta} \varepsilon_{\gamma\theta}^* + p_{\alpha\gamma\theta\theta} \kappa_{\gamma\theta\theta}^*) (G_{\alpha\beta,\kappa} + G_{\alpha\kappa,\beta}) \right. \\ & \left. - (h_{\alpha\gamma\theta} \varepsilon_{\gamma\theta}^* + d_{\alpha\gamma\theta\theta} \kappa_{\gamma\theta\theta}^*) (G_{\alpha\beta,\eta\kappa} + G_{\alpha\kappa,\eta\beta}) n_\eta \right] dS_y. \end{aligned} \quad (34)$$

From Eq. (34) it follows that

$$S_{\beta\kappa\gamma\theta}^F = S_{\beta\kappa\gamma\theta}^\infty + S_{\beta\kappa\gamma\theta}^{B,F}, \quad T_{\beta\kappa\gamma\theta\chi}^F = T_{\beta\kappa\gamma\theta\chi}^\infty + T_{\beta\kappa\gamma\theta\chi}^{B,F}, \quad (35a, b)$$

where

$$\begin{aligned} S_{\beta\kappa\gamma\theta}^{B,F} & \equiv \frac{1}{2} \int_{\partial R} \left[g_{\alpha\gamma\theta} (G_{\alpha\beta,\kappa} + G_{\alpha\kappa,\beta}) - h_{\alpha\gamma\theta} (G_{\alpha\beta,\eta\kappa} + G_{\alpha\kappa,\eta\beta}) n_\eta \right] dS_y, \\ T_{\beta\kappa\gamma\theta\chi}^{B,F} & \equiv \frac{1}{2} \int_{\partial R} \left[p_{\alpha\gamma\theta\chi} (G_{\alpha\beta,\kappa} + G_{\alpha\kappa,\beta}) - d_{\alpha\gamma\theta\chi} (G_{\alpha\beta,\eta\kappa} + G_{\alpha\kappa,\eta\beta}) n_\eta \right] dS_y. \end{aligned} \quad (36b)$$

Note that $S_{\beta\kappa\gamma\theta}^{B,F}$ and $T_{\beta\kappa\gamma\theta\chi}^{B,F}$, as defined in Eqs. (35a,b) and (36a,b), can be regarded, respectively, as the boundary parts of the finite-domain Eshelby tensor and Eshelby-like tensor. In the absence of the boundary effect, $S_{\beta\kappa\gamma\theta}^{B,F} = 0$ and $T_{\beta\kappa\gamma\theta\chi}^{B,F} = 0$, which follow from the fact that the first- and second-order derivatives of the Green's function with respect to r vanish at infinity (i.e., as $r \rightarrow \infty$) (see Eqs. (9) and (10a,b)). As a result, $S_{\beta\kappa\gamma\theta}^F$ and $T_{\beta\kappa\gamma\theta\chi}^F$ reduce, respectively, to their counterparts $S_{\beta\kappa\gamma\theta}^\infty$ and $T_{\beta\kappa\gamma\theta\chi}^\infty$ for the unbounded-domain plane strain inclusion problem, as shown in Eqs. (35a,b).

Clearly, Eqs. (35a,b), (36a,b), (30b,c) and (33a–d) define the integral equations to solve for $S_{\beta\kappa\gamma\theta}^F$ and $T_{\beta\kappa\gamma\theta\chi}^F$, which depend on the shape and size of both the elastic body (through the line integrals listed in Eqs. (36a) and (36b)) and the inclusion (via $S_{\beta\kappa\gamma\theta}^\infty$ and $T_{\beta\kappa\gamma\theta\chi}^\infty$ given in Eqs. (30b) and (30c)). Hence, closed-form solutions may be derived only for finite-domain plane strain inclusion problems with simple-shape finite elastic bodies and inclusions. The problem with a plane strain inclusion of circular cross section to be discussed in the next section is one of such problems that have been solved analytically.

3. Eshelby tensor for a finite-domain cylindrical inclusion problem

3.1. Position-dependent Eshelby tensor

Consider a plane strain cylindrical elastic body with a circular cross section R of radius H containing a concentric cylindrical inclusion having a circular cross section R_I of radius a , as illustrated in Fig. 3.

For the unbounded cylindrical inclusion problem, the Eshelby tensor *inside* the inclusion based on the SSGT is given by (Ma and Gao, 2010a)

$$S_{\beta\kappa\gamma\theta}^{I,\infty}(\mathbf{x}) = S_{\beta\kappa\gamma\theta}^{I,C} + S_{\beta\kappa\gamma\theta}^{I,G}(\mathbf{x}), \quad (37)$$

where \mathbf{x} is a point located inside the inclusion (i.e., $\mathbf{x} \in R_I$ or $0 < |\mathbf{x}| < a$), $S_{\beta\kappa\gamma\theta}^{I,C}$ is the classical part that is uniform for all $\mathbf{x} \in R_I$, and $S_{\beta\kappa\gamma\theta}^{I,G}(\mathbf{x})$ is the gradient part that varies with the position of point \mathbf{x} . It can be readily shown that $S_{\beta\kappa\gamma\theta}^{I,\infty}$ obtained in Ma and Gao (2010a) and involved in Eq. (37) can be written in a matrix form as

$$S_{\beta\kappa\gamma\theta}^{I,\infty}(\mathbf{x}) = [\Theta_{\beta\kappa\gamma\theta}(\mathbf{x}^0)]^T [S_{\beta\kappa\gamma\theta}^{I,\infty}(\mathbf{x})], \quad (38)$$

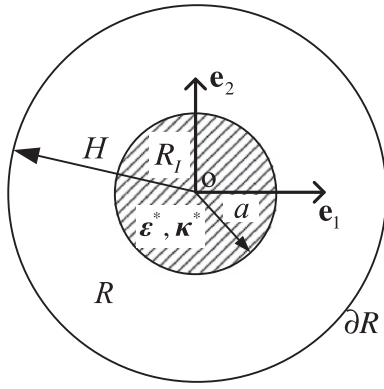


Fig. 3. Cylindrical inclusion in a finite cylindrical elastic body.

where

$$[\Theta_{\beta\kappa\gamma\theta}(\mathbf{x}^0)]^T = [\delta_{\beta\kappa}\delta_{\gamma\theta}, \delta_{\beta\gamma}\delta_{\kappa\theta} + \delta_{\beta\theta}\delta_{\kappa\gamma}, \delta_{\beta\kappa}x_\gamma^0x_\theta^0, \delta_{\gamma\theta}x_\beta^0x_\kappa^0, \delta_{\beta\gamma}x_\kappa^0x_\theta^0, \delta_{\beta\theta}x_\kappa^0x_\gamma^0 + \delta_{\kappa\gamma}x_\beta^0x_\theta^0 + \delta_{\kappa\theta}x_\beta^0x_\gamma^0, x_\beta^0x_\kappa^0x_\gamma^0x_\theta^0], \quad (39a)$$

$$[S^{I,\infty}(\mathbf{x})] = [S^{I,C}(\mathbf{x})] + [S^{I,G}(\mathbf{x})], \quad (39b)$$

$$[S^{I,C}(\mathbf{x})] = \left[\frac{4\nu-1}{8(1-\nu)}, \frac{3-4\nu}{8(1-\nu)}, 0, 0, 0, 0 \right]^T, \quad (39c)$$

$$[S^{I,G}(\mathbf{x})] = [S_1^{I,G}, S_2^{I,G}, S_3^{I,G}, S_4^{I,G}, S_5^{I,G}, S_6^{I,G}]^T, \quad (39d)$$

with

$$\begin{aligned} S_1^{I,G} &= \frac{aK_1}{(1-\nu)x^3} [LxI_0 - (\nu x^2 + 2L^2)I_1], \\ S_2^{I,G} &= \frac{aK_1}{(1-\nu)x^3} [LxI_0 + (-x^2 + \nu x^2 - 2L^2)I_1], \\ S_3^{I,G} &= \frac{aK_1}{(1-\nu)x^3} [-4LxI_0 + (x^2 + 8L^2)I_1], \\ S_4^{I,G} &= \frac{aK_1}{(1-\nu)x^3L} [-x(\nu x^2 + 4L^2)I_0 + L(x^2 + 2\nu x^2 + 8L^2)I_1], \\ S_5^{I,G} &= \frac{aK_1}{2(1-\nu)x^3L} [-x(x^2 - \nu x^2 + 8L^2)I_0 + 2L(2x^2 - \nu x^2 + 8L^2)I_1], \\ S_6^{I,G} &= \frac{aK_1}{(1-\nu)x^3L} [x(x^2 + 24L^2)I_0 - 8L(x^2 + 6L^2)I_1]. \end{aligned} \quad (40a-f)$$

In Eq. (39a) and throughout this paper, $x_\alpha^0 = x_\alpha/x$ is the α th component of the unit vector $\mathbf{x}^0 = \mathbf{x}/x$ in the x_1x_2 -plane, and $x = |\mathbf{x}| = \sqrt{x_1^2 + x_2^2}$ is the distance from point \mathbf{x} to the origin of the coordinate system which coincides with the center of the circular cross section. In Eqs. (40a–f), $I_0 = I_0(\frac{x}{L})$, $I_1 = I_1(\frac{x}{L})$ and $K_1 = K_1(\frac{a}{L})$ are modified Bessel functions of the indicated arguments, with $x < a$.

For the unbounded cylindrical inclusion problem, the Eshelby tensor outside the inclusion based on the SSGT has been obtained as (Ma and Gao, 2010a)

$$S_{\beta\kappa\gamma\theta}^{E,\infty}(\mathbf{x}) = S_{\beta\kappa\gamma\theta}^{E,C}(\mathbf{x}) + S_{\beta\kappa\gamma\theta}^{E,G}(\mathbf{x}), \quad (41)$$

where \mathbf{x} is a point located outside the inclusion (i.e., $\mathbf{x} \notin R_i$ or $a < x < H$), $S_{\beta\kappa\gamma\theta}^{E,C}(\mathbf{x})$ is the classical part, and $S_{\beta\kappa\gamma\theta}^{E,G}(\mathbf{x})$ is the gradient part. Both $S_{\beta\kappa\gamma\theta}^{E,C}$ and $S_{\beta\kappa\gamma\theta}^{E,G}$ vary with the position of \mathbf{x} in this exterior case, unlike in the interior case. In a matrix form, Eq. (41) can be written as

$$S_{\beta\kappa\gamma\theta}^{E,\infty}(\mathbf{x}) = [\Theta_{\beta\kappa\gamma\theta}(\mathbf{x}^0)]^T [S^{E,\infty}(\mathbf{x})], \quad (42)$$

where $[\Theta_{\beta\kappa\gamma\theta}(\mathbf{x}^0)]^T$ is the same as that defined in Eq. (39a), and

$$[S^{E,\infty}(\mathbf{x})] = [S^{E,C}(\mathbf{x})] + [S^{E,G}(\mathbf{x})], \quad (43)$$

in which

$$[S^{E,C}(\mathbf{x})] = \frac{a^2}{8(1-\nu)x^4} [4\nu x^2 - 2x^2 + a^2, -4\nu x^2 + 2x^2 + a^2, 4(x^2 - a^2), -4(2\nu x^2 - x^2 + a^2), 4(\nu x^2 - a^2), 8(3a^2 - 2x^2)], \quad (44a)$$

$$S^{E,G}(\mathbf{x}) = [S_1^{E,G}, S_2^{E,G}, S_3^{E,G}, S_4^{E,G}, S_5^{E,G}, S_6^{E,G}]^T, \quad (44b)$$

with

$$S_1^{E,G} = -\frac{aI_1}{(1-\nu)x^3} [LxK_0 + (\nu x^2 + 2L^2)K_1] + \frac{L^2a^2}{(1-\nu)x^4}, \quad (45a)$$

$$\begin{aligned} S_2^{E,G} &= \frac{aI_1}{(1-\nu)x^3} [-LxK_0 + (-x^2 + \nu x^2 - 2L^2)K_1] \\ &+ \frac{L^2a^2}{(1-\nu)x^4}, \end{aligned} \quad (45b)$$

$$S_3^{E,G} = \frac{aI_1}{(1-\nu)x^3} [4LxK_0 + (x^2 + 8L^2)K_1] - \frac{4L^2a^2}{(1-\nu)x^4}, \quad (45c)$$

$$S_4^{E,G} = \frac{aI_1}{(1-\nu)x^3L} [x(\nu x^2 + 4L^2)K_0 + L(x^2 + 2\nu x^2 + 8L^2)K_1] - \frac{4L^2a^2}{(1-\nu)x^4}, \quad (45d)$$

$$\begin{aligned} S_5^{E,G} &= \frac{aI_1}{2(1-\nu)x^3L} [x(x^2 - \nu x^2 + 8L^2)K_0 + 2L(2x^2 - \nu x^2 + 8L^2)K_1] \\ &- \frac{4L^2a^2}{(1-\nu)x^4}, \end{aligned} \quad (45e)$$

$$\begin{aligned} S_6^{E,G} &= -\frac{aI_1}{(1-\nu)x^3L} [x(x^2 + 24L^2)K_0 + 8L(x^2 + 6L^2)K_1] \\ &+ \frac{24L^2a^2}{(1-\nu)x^4}. \end{aligned} \quad (45f)$$

In Eqs. (45a–f), $I_1 = I_1(\frac{x}{L})$, $K_0 = K_0(\frac{x}{L})$ and $K_1 = K_1(\frac{a}{L})$ are modified Bessel functions of the indicated arguments, with $x > a$. As shown in Ma and Gao (2010a), when the gradient effect is suppressed by letting $L = 0$, the gradient part of the Eshelby tensor in both the interior and exterior regions given respectively in Eqs. (39d), (40a–f) and Eqs. (44b), (45a)–(45f) vanishes, and the SSGT-based Eshelby tensor for the unbounded-domain cylindrical inclusion problem reduces to that obtained using classical elasticity.

Based on the similarity between the unbounded- and bounded-domain inclusion problems and the forms of the Eshelby tensor for the unbounded-domain problem given in Eqs. (38) and (42), it is postulated that the Eshelby tensor for the current bounded-domain cylindrical inclusion problem can be expressed in a similar form as

$$S_{\beta\kappa\gamma\theta}^{E,F}(\mathbf{x}) = [\Theta_{\beta\kappa\gamma\theta}(\mathbf{x}^0)]^T [S^{E,F}(\mathbf{x})], \quad (46)$$

where $[\Theta_{\beta\kappa\gamma\theta}(\mathbf{x}^0)]^T$ is the same as that defined in Eq. (39a), and

$$[S^{E,F}(\mathbf{x})] = [S_1^{E,F}(\mathbf{x}), S_2^{E,F}(\mathbf{x}), S_3^{E,F}(\mathbf{x}), S_4^{E,F}(\mathbf{x}), S_5^{E,F}(\mathbf{x}), S_6^{E,F}(\mathbf{x})]^T \quad (47)$$

is an array of six components yet to be determined.

Using Eq. (46) in Eqs. 33a and 33c yields, after carrying out the algebra, on ∂R ,

$$g_{x\gamma\theta} = [\Xi_{x\gamma\theta}] [S^{EF}(H)], \quad h_{x\gamma\theta} = 0, \quad (48a, b)$$

where

$$[\Xi_{x\gamma\theta}] \equiv [\delta_{\gamma\theta} n_x, \delta_{x\gamma} n_\theta + \delta_{x\theta} n_\gamma, n_x n_\gamma n_\theta] [M]^T, \quad (49)$$

$$[M] = \begin{bmatrix} 2\lambda + 2\mu & 0 & 0 \\ 2\lambda & 2\mu & 0 \\ -4\alpha(\lambda + \mu) & 0 & 2(\lambda + \mu)(1 + 4\alpha) \\ \lambda + 2\mu + 4\mu\alpha & 0 & 0 \\ -8\lambda\alpha & 2\mu & 4(\lambda + \mu)(1 + 4\alpha) \\ -2(\lambda + 2\mu)\alpha & -4\mu\alpha & \lambda + 2\mu + 4(\lambda + 5\mu)\alpha \end{bmatrix} \quad (50)$$

with $\alpha \equiv L^2/H^2$, λ and μ being the Lamé constants, $n_\alpha = y_\alpha/y$ being the α th component of the unit vector \mathbf{n} representing the direction of \mathbf{y} , and $y = |\mathbf{y}| = \sqrt{y_1^2 + y_2^2}$.

Using Eqs. (48a,b)–(50) in Eq. (36a) gives the boundary part of the finite-domain Eshelby tensor, in a matrix form, as

$$S_{\beta\kappa\gamma\theta}^{B,F} = \frac{1}{2} [Q_1, Q_2, Q_3] [M]^T [S^{EF}(H)], \quad (51)$$

where

$$\begin{aligned} Q_1 &= \int_{\partial R} \delta_{\gamma\theta} n_x (G_{\alpha\beta,\kappa} + G_{\alpha\kappa,\beta}) dS_y, \quad Q_2 \\ &= \int_{\partial R} (\delta_{x\gamma} n_\theta + \delta_{x\theta} n_\gamma) (G_{\alpha\beta,\kappa} + G_{\alpha\kappa,\beta}) dS_y, \quad Q_3 \\ &= \int_{\partial R} n_x n_\gamma n_\theta (G_{\alpha\beta,\kappa} + G_{\alpha\kappa,\beta}) dS_y, \end{aligned} \quad (52)$$

with $G_{\alpha\beta}$, given in Eqs. (12) and (13a,b), being the plane strain Green's function based on the SSGET. The use of Eqs. (12) and (13a,b) in Eq. (52) results in

$$Q_1 = \delta_{\gamma\theta} \left(\langle n_\beta A(r) \rangle_{,\kappa} + \langle n_\kappa A(r) \rangle_{,\beta} + 2 \langle n_x B(r) \rangle_{,\alpha\beta\kappa} \right), \quad (53a)$$

$$\begin{aligned} Q_2 &= \delta_{\gamma\beta} \langle n_\theta A(r) \rangle_{,\kappa} + \delta_{\gamma\kappa} \langle n_\theta A(r) \rangle_{,\beta} + \delta_{\theta\beta} \langle n_x A(r) \rangle_{,\kappa} \\ &\quad + \delta_{\theta\kappa} \langle n_x A(r) \rangle_{,\beta} + 2 \langle n_\theta B(r) \rangle_{,\gamma\beta\kappa} + 2 \langle n_\gamma B(r) \rangle_{,\theta\beta\kappa}, \end{aligned} \quad (53b)$$

$$Q_3 = \langle n_\beta n_\gamma n_\theta A(r) \rangle_{,\kappa} + \langle n_\kappa n_\gamma n_\theta A(r) \rangle_{,\beta} + 2 \langle n_x n_\gamma n_\theta B(r) \rangle_{,\alpha\beta\kappa}, \quad (53c)$$

where $r = |\mathbf{x} - \mathbf{y}|$, and $A(r)$ and $B(r)$ are defined in Eqs. (13a,b). In Eqs. (53a)–(53c) and in the sequel, $\langle f \rangle$ denotes the line integral of function f along ∂R (i.e., the circle enclosing the cross section of the cylindrical elastic matrix of radius H , as shown in Fig. 4) defined by

$$\langle f \rangle = \int_{\partial R} f dS_y. \quad (54)$$

The integrals in Eqs. (53a)–(53c) can be analytically evaluated with the help of the following relations (see Appendix B):

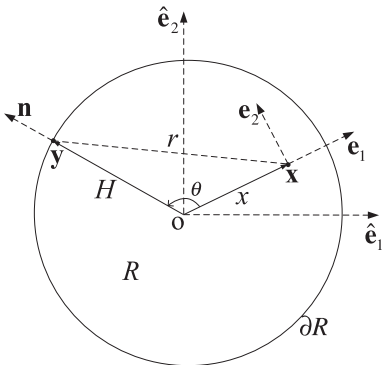


Fig. 4. Locations of $\mathbf{x} (\in R)$ and $\mathbf{y} (\in \partial R)$.

$$\langle f(r) n_x \rangle = f_0(x) x_x, \quad (55)$$

$$\langle f(r) n_x n_\beta n_\gamma \rangle = f_1(x) (x_x \delta_{\beta\gamma} + x_\beta \delta_{x\gamma} + x_\gamma \delta_{x\beta}) + f_2(x) x_x x_\beta x_\gamma, \quad (56)$$

where

$$\begin{aligned} f_0(x) &= \frac{H}{x} \int_0^{2\pi} f(r) \cos \theta d\theta, \quad f_1(x) \\ &= \frac{H}{x} \int_0^{2\pi} f(r) (\cos \theta - \cos^3 \theta) d\theta, \end{aligned} \quad (57a, b)$$

$$f_2(x) = \frac{H}{x^3} \int_0^{2\pi} f(r) (4 \cos^3 \theta - 3 \cos \theta) d\theta, \quad (57c)$$

with

$$r = |\mathbf{x} - \mathbf{y}| = \sqrt{x^2 + H^2 - 2xH \cos \theta}, \quad (57d)$$

in which H is the radius of the circle ∂R , θ is the angle between $\mathbf{x} (\in R)$ and $\mathbf{y} (\in \partial R)$, as shown in Fig. 4. Clearly, Eq. (57d) follows directly from the cosine law.

Applying Eqs. (55) and (57a) to $A(r)$ and $B(r)$ defined in Eqs. (13a,b), respectively, yields, together with Eq. (54),

$$\langle A(r) n_x \rangle = A_0(x) x_x, \quad \langle B(r) n_x \rangle = B_0(x) x_x, \quad (58a, b)$$

where

$$\begin{aligned} A_0(x) &= \frac{1}{2\mu} \left(1 - \frac{2I_1 K_1}{\zeta} \right), \quad B_0(x) \\ &= -\frac{H^2}{16\mu(1-\nu)} \left(2 \ln H + \frac{1}{2} \zeta^2 \right) - \frac{L^2}{2(1-\nu)} A_0(x). \end{aligned} \quad (59a, b)$$

Similarly, the application of Eqs. (56) and (57b,c) to $A(r)$ and $B(r)$ respectively results in

$$\begin{aligned} \langle A(r) n_x n_\beta n_\gamma \rangle &= A_1(x) (x_x \delta_{\beta\gamma} + x_\beta \delta_{x\gamma} + x_\gamma \delta_{x\beta}) \\ &\quad + A_2(x) x_x x_\beta x_\gamma, \\ \langle B(r) n_x n_\beta n_\gamma \rangle &= B_1(x) (x_x \delta_{\beta\gamma} + x_\beta \delta_{x\gamma} + x_\gamma \delta_{x\beta}) \\ &\quad + B_2(x) x_x x_\beta x_\gamma, \end{aligned} \quad (60a, b)$$

where

$$A_1(x) = \frac{1}{24\mu} \left[3 - \zeta^2 - \frac{6}{\zeta} (I_1 K_1 - I_3 K_3) \right], \quad (61a)$$

$$\begin{aligned} B_1(x) &= -\frac{H^2}{768\mu(1-\nu)} (8\zeta^2 - \zeta^4 + 24 \ln H) \\ &\quad - \frac{L^2}{2(1-\nu)} A_1(x), \end{aligned} \quad (61b)$$

$$\begin{aligned} A_2(x) &= \frac{1}{6\mu\zeta^2 H^2} \left(\zeta^2 - \frac{6}{\zeta} I_3 K_3 \right), \quad B_2(x) \\ &= \frac{1}{192\mu(1-\nu)} (2 - \zeta^2) - \frac{L^2}{2(1-\nu)} A_2(x). \end{aligned} \quad (61c, d)$$

In Eqs. (59a,b) and (61a–d), $\zeta \equiv \frac{x}{H}$, and $I_1 = I_1(\frac{x}{H})$, $I_3 = I_3(\frac{x}{H})$, $K_1 = K_1(\frac{x}{H})$ and $K_3 = K_3(\frac{x}{H})$ are modified Bessel functions of the indicated arguments, with $x < H$. Note that in reaching Eqs. (59a,b) and (61a–d) use has been made of the following identities:

$$\int_0^{2\pi} \ln(1 + \zeta^2 - 2\zeta \cos \theta) d\theta = 0, \quad (62a)$$

$$\int_0^\pi \ln(1 + \zeta^2 - 2\zeta \cos \theta) \cos(2\theta) \cos \theta d\theta = -\frac{\pi}{2} \left(\frac{\zeta^3}{3} + \zeta \right), \quad (62b)$$

$$\int_0^\pi \ln(1 + \zeta^2 - 2\zeta \cos \theta) \cos(n\theta) d\theta = -\frac{\pi}{n} \zeta^n \quad (n = 1, 2, \dots), \quad (62c)$$

where $0 < \xi < 1$ (Gradshteyn and Ryzhik, 2007), and

$$K_0\left(\frac{r}{L}\right) = I_0\left(\frac{x}{L}\right)K_0\left(\frac{H}{L}\right) + 2 \sum_{n=1}^{\infty} I_n\left(\frac{x}{L}\right)K_n\left(\frac{H}{L}\right) \cos(n\theta) \quad (x < H), \quad (62d)$$

where r is define in Eq. (57d) (Magnus et al., 1966).

Using Eqs. (58a,b)–(61a–d) in Eqs. (53a)–(53c) then leads to, in a matrix form,

$$[Q_1, Q_2, Q_3] = [\Theta_{\beta\kappa\gamma\theta}(\mathbf{x}^0)]^T [Q(x)]^T, \quad (63)$$

where $[\Theta_{\beta\kappa\gamma\theta}(\mathbf{x}^0)]^T$ is the same as that listed in Eq. (39a), and $[Q(x)]$ is a 3 by 6 matrix whose components are given by

$$\begin{aligned} Q_{11} &= 2[A_0 + D_1(N)], \quad Q_{14} = 2x^2[D_1(A_0) + D_2(N)], \\ Q_{12} &= Q_{13} = Q_{15} = Q_{16} = 0, \\ Q_{21} &= 4D_1(B_0), \quad Q_{22} = 2A_0 + 4D_1(B_0), \\ Q_{23} &= 4x^2D_2(B_0), \quad Q_{24} = Q_{23}, \\ Q_{25} &= x^2[D_1(A_0) + 4D_2(B_0)], \quad Q_{26} = 4x^4D_3(B_0), \\ Q_{31} &= 2[A_1 + D_1(Z) + 2D_1(B_1)], \\ Q_{32} &= 2[A_1 + X + 2D_1(B_1)], \\ Q_{33} &= 2x^2[A_2 + 2D_2(B_1) + D_1(X)], \\ Q_{34} &= 2x^2[D_1(A_1) + D_2(Z) + 2D_2(B_1)], \\ Q_{35} &= x^2[A_2 + D_1(A_1) + 2D_1(X) + 4D_2(B_1)], \\ Q_{36} &= 2x^4[D_1(A_2) + D_2(X) + 2D_3(B_1)], \end{aligned} \quad (64)$$

with

$$N(x) \equiv xB'_0 + 2B_0, \quad Z(x) \equiv xB'_1 + 2B_1, \quad X(x) \equiv xB'_2 + 4B_2. \quad (65)$$

The differential operators $D_1(\cdot)$, $D_2(\cdot)$ and $D_3(\cdot)$ involved in Eq. (64) are defined by

$$\begin{aligned} D_1(F) &= \frac{F'}{x}, \quad D_2(F) = \frac{1}{x^2} \left(F'' - \frac{F'}{x} \right), \\ D_3(F) &= \frac{1}{x^3} \left(F''' - \frac{3F''}{x} + \frac{3F'}{x^2} \right), \end{aligned} \quad (66)$$

where $F(x)$ is a sufficiently smooth function of x . The superscripts “’”, “’’” and “'''” in Eqs. (65) and (66) denote, respectively, the first, second and third derivatives with respect to x .

Substituting Eq. (63) into Eq. (51) then yields the boundary part of the finite-domain Eshelby tensor as

$$S_{\beta\kappa\gamma\theta}^{B,F}(\mathbf{x}) = \frac{1}{2} [\Theta_{\beta\kappa\gamma\theta}(\mathbf{x}^0)]^T [Q(x)]^T [M]^T [S^{E,F}(H)], \quad (67)$$

where $[Q(x)]$ is the 3 by 6 matrix whose components are listed in Eq. (64), $[M]$ is given in Eq. (50), and $[S^{E,F}(H)]$ can be determined as follows.

Note that Eq. (67) can be rewritten as

$$S_{\beta\kappa\gamma\theta}^{B,F}(\mathbf{x}) = [\Theta_{\beta\kappa\gamma\theta}(\mathbf{x}^0)]^T [K(x)] [S^{E,F}(H)], \quad (68)$$

where

$$[K(x)] \equiv \frac{1}{2} [Q(x)]^T [M]^T \quad (69)$$

is a six by six matrix. When the gradient effect is not considered, $L = 0$ (so that $x/L \rightarrow \infty$, $H/L \rightarrow \infty$), and Eqs. (59a,b) and (61a–d) reduce to

$$\begin{aligned} A_0(x) &= \frac{1}{2\mu}, \quad A_1(x) = \frac{3 - \zeta^2}{24\mu}, \quad A_2(x) = \frac{1}{6\mu H^2}, \quad B_0(x) \\ &= -\frac{H^2}{16\mu(1-\nu)} \left(2\ln H + \frac{1}{2}\zeta^2 \right), \end{aligned}$$

$$\begin{aligned} B_1(x) &= -\frac{H^2}{768\mu(1-\nu)} (8\zeta^2 - \zeta^4 + 24\ln H), \\ B_2(x) &= \frac{1}{192\mu(1-\nu)} (2 - \zeta^2), \end{aligned} \quad (70a-f)$$

where $\zeta \equiv x/H$ and use has been made of the results: $I_1K_1 \rightarrow 0$, $I_3K_3 \rightarrow 0$ as $L = 0$, which are obtained from the following asymptotic relation (e.g., Arfken and Weber, 2005) as well as that given in Eq. (10c):

$$I_n(z) \sim \frac{1}{\sqrt{2\pi z}} e^z \quad \text{as } z \rightarrow \infty. \quad (70g)$$

The classical counterparts of $[Q]$ and $[M]$ matrices can be obtained, respectively, by using Eqs. (70a–f) in Eq. (64) and $\alpha = 0$ in Eq. (50). Substituting the resulting $[Q]$ and $[M]$ matrices into Eq. (69) will then lead to the $[K]$ matrix based on the classical elasticity, which can be shown to be equivalent to that provided in Li et al. (2005) using a different representation.

Using Eqs. (38), (42), (46) and (68) in Eq. (35a) gives, noting that the six components of $[\Theta_{\beta\kappa\gamma\theta}(\mathbf{x}^0)]^T$ are linearly independent,

$$[S^{L,F}(x)] = [S^{L,\infty}(x)] + [K(x)][S^{E,F}(H)] \quad (71)$$

for the interior case with $0 < x < a$, and

$$[S^{E,F}(x)] = [S^{E,\infty}(x)] + [K(x)][S^{E,F}(H)] \quad (72)$$

for the exterior case with $a < x < H$. By setting $x \rightarrow H$, Eq. (72) gives

$$[S^{E,F}(H)] = [I - K(H)]^{-1} [S^{E,\infty}(H)], \quad (73)$$

where $[I]$ is the six by six identity matrix, $[K(H)]$ is obtainable from Eq. (69), and $[S^{E,\infty}(H)]$ is available from Eqs. (43)–(45a–f) with $x = H$.

Finally, it follows from Eqs. (39b), (46), (71) and (73) that the Eshelby tensor inside the cylindrical inclusion for the current finite-domain inclusion problem can be expressed as

$$S_{\beta\kappa\gamma\theta}^{L,F}(\mathbf{x}) = [\Theta_{\beta\kappa\gamma\theta}(\mathbf{x}^0)]^T \{ [S^{L,C}] + [S^{L,G}(x)] + [S^{B,F}(x)] \}, \quad (74)$$

with

$$[S^{B,F}(x)] \equiv [K(x)][I - K(H)]^{-1} [S^{E,\infty}(H)], \quad (75)$$

where $\mathbf{x} \in R_i$, $0 < x < a$, and $[S^{L,C}]$, $[S^{L,G}]$ and $[S^{B,F}]$ are, respectively, the classical, gradient and boundary parts of the Eshelby tensor inside the inclusion based on the SSGT. Note that $[S^{L,C}]$, as given in Eq. (39c), is uniform inside the inclusion, while $[S^{L,G}]$, as listed in Eqs. (39d) and (40a–f), depends on L , a and x in a complicated manner. In addition, $[S^{B,F}]$ given in Eq. (75) varies with L , a , H and x . That is, $[S^{B,F}]$ is non-uniform inside the inclusion and is different for the elastic body with different body and/or inclusion sizes (i.e., with varying H and/or a) and different materials (with changing L).

The Eshelby-like tensor $T_{\beta\kappa\gamma\theta\chi}^{L,F}(\mathbf{x})$, given in Eqs. (30c), (35b) and (36b), can be obtained for this finite-domain cylindrical inclusion problem by following a procedure similar to that used in deriving the Eshelby tensor $S_{\beta\kappa\gamma\theta}^{L,F}(\mathbf{x})$. After some lengthy derivations, $T_{\beta\kappa\gamma\theta\chi}^{L,F}(\mathbf{x})$ is found to have the matrix form:

$$T_{\beta\kappa\gamma\theta\chi}^{L,F}(\mathbf{x}) = [\Xi_{\beta\kappa\gamma\theta\chi}(\mathbf{x}^0)]^T [T^{L,F}(x)], \quad (76)$$

where

$$\begin{aligned} [\Xi_{\beta\kappa\gamma\theta\chi}(\mathbf{x}^0)]^T &= [\delta_{\gamma\theta} (x_\beta^0 \delta_{\kappa\chi} + x_\kappa^0 \delta_{\beta\chi}), \delta_{\beta\kappa} (x_\gamma^0 \delta_{\theta\chi} + x_\theta^0 \delta_{\gamma\chi}), \\ &\quad \delta_{\gamma\theta} x_\beta^0 x_\kappa^0, \delta_{\beta\kappa} x_\gamma^0 x_\theta^0, \delta_{\theta\chi} (x_\beta^0 \delta_{\gamma\chi} + x_\gamma^0 \delta_{\beta\chi}), \\ &\quad + \delta_{\gamma\chi} (x_\kappa^0 \delta_{\beta\theta} + x_\beta^0 \delta_{\kappa\theta}), \delta_{\beta\chi} (x_\gamma^0 \delta_{\kappa\theta} + x_\theta^0 \delta_{\kappa\gamma}), \\ &\quad + \delta_{\kappa\chi} (x_\gamma^0 \delta_{\beta\theta} + x_\theta^0 \delta_{\beta\gamma}), x_\chi^0 (\delta_{\beta\gamma} x_\kappa^0 x_\theta^0 + \delta_{\beta\theta} x_\kappa^0 x_\gamma^0 + \delta_{\kappa\gamma} x_\beta^0 x_\theta^0 \\ &\quad + \delta_{\kappa\theta} x_\beta^0 x_\gamma^0), x_\chi^0 (\delta_{\beta\gamma} \delta_{\kappa\theta} + \delta_{\beta\theta} \delta_{\kappa\gamma}), x_\beta^0 x_\kappa^0 (x_\gamma^0 \delta_{\theta\chi} + x_\theta^0 \delta_{\gamma\chi}), \\ &\quad x_\gamma^0 x_\theta^0 (x_\beta^0 \delta_{\kappa\chi} + x_\kappa^0 \delta_{\beta\chi}), x_\chi^0 \delta_{\beta\kappa} \delta_{\gamma\theta}, x_\chi^0 x_\beta^0 x_\kappa^0 x_\gamma^0 x_\theta^0], \end{aligned} \quad (77)$$

and $[T^F(x)]$ is an array with 12 components which are functions of x . Since the average of $T^F_{\beta\kappa\gamma\theta\chi}(\mathbf{x})$ over the cylindrical inclusion vanishes, as will be shown next, detailed expressions of $[T^F(x)]$ will not be discussed further.

3.2. Averaged Eshelby tensor

Considering that the finite-domain Eshelby tensor \mathbf{S}^{LF} is position-dependent inside the inclusion, the average of \mathbf{S}^{LF} over the circular cross section of the cylindrical inclusion will be needed in homogenization analyses of fiber-reinforced composites. Hence, the area average of \mathbf{S}^{LF} is evaluated here.

The area average of a sufficiently smooth function $F(\mathbf{x})$ over the circular cross section R_l of the inclusion is defined by

$$\langle F(\mathbf{x}) \rangle_A = \frac{1}{\text{Area}(R_l)} \int \int_{R_l} F(\mathbf{x}) dA = \frac{1}{\pi a^2} \int_0^a \int_0^{2\pi} F(\mathbf{x}) x d\theta dx, \quad (78)$$

where use has been made of the area element $dA = x d\theta dx$ in a polar coordinate system, with x being the (radial) distance from point \mathbf{x} to the origin of the coordinate system (i.e., the center of the circular cross section R).

Note that in the polar coordinate system adopted here,

$$x_1^0 = \cos \theta, \quad x_2^0 = \sin \theta. \quad (79)$$

It then follows from Eq. (79) that

$$\int_0^{2\pi} x_\alpha^0 x_\beta^0 d\theta = \pi \delta_{\alpha\beta}, \quad \int_0^{2\pi} x_\alpha^0 x_\beta^0 x_\gamma^0 x_\delta^0 d\theta = \frac{\pi}{4} (\delta_{\alpha\beta} \delta_{\gamma\delta} + \delta_{\alpha\gamma} \delta_{\beta\delta} + \delta_{\alpha\delta} \delta_{\beta\gamma}),$$

$$\int_0^{2\pi} x_\alpha^0 d\theta = 0, \quad \int_0^{2\pi} x_\alpha^0 x_\beta^0 x_\gamma^0 d\theta = 0, \quad \int_0^{2\pi} x_\alpha^0 x_\beta^0 x_\gamma^0 x_\delta^0 x_\epsilon^0 d\theta = 0. \quad (80a-e)$$

Replacing $F(\mathbf{x})$ in Eq. (78) with $S^{LF}_{\alpha\beta\gamma\theta}(\mathbf{x})$ given in Eq. (74) then leads to, with the help of Eqs. (39a) and (80a,b),

$$\langle S^{LF}_{\alpha\beta\gamma\theta} \rangle_A = \langle S^{L,\infty}_{\alpha\beta\gamma\theta} \rangle_A + \langle S^{B,F}_{\alpha\beta\gamma\theta} \rangle_A, \quad (81)$$

where the area-averaged Eshelby tensor for the unbounded cylindrical inclusion problem has been obtained in a closed form in Ma and Gao (2010a) as

$$\langle S^{L,\infty}_{\alpha\beta\gamma\theta} \rangle_A = \frac{1}{8(1-\nu)} \left[1 - 2K_1 \left(\frac{a}{L} \right) I_1 \left(\frac{a}{L} \right) \right] [(4\nu - 1) \delta_{\alpha\beta} \delta_{\gamma\theta} + (3 - 4\nu) (\delta_{\alpha\gamma} \delta_{\beta\theta} + \delta_{\alpha\theta} \delta_{\beta\gamma})], \quad (82)$$

and the area-averaged boundary part of the Eshelby tensor for the bounded cylindrical inclusion problem is given by

$$\langle S^{B,F}_{\alpha\beta\gamma\theta} \rangle_A = S_1(a, L, H) \delta_{\alpha\beta} \delta_{\gamma\theta} + S_2(a, L, H) (\delta_{\alpha\gamma} \delta_{\beta\theta} + \delta_{\alpha\theta} \delta_{\beta\gamma}), \quad (83)$$

with

$$S_1 = \frac{1}{a^2} \left(2\overline{S}_1^{B,F} + \overline{S}_3^{B,F} + \overline{S}_4^{B,F} + \frac{1}{4}\overline{S}_6^{B,F} \right), \quad S_2 = \frac{1}{a^2} \left(2\overline{S}_2^{B,F} + 2\overline{S}_5^{B,F} + \frac{1}{4}\overline{S}_6^{B,F} \right), \quad (84a, b)$$

$$\overline{S}_n^{B,F} \equiv \int_0^a x S_n^{B,F}(x) dx, \quad (84c)$$

in which $S_n^{B,F}(x) (n = 1, 2, \dots, 6)$ is the n th component of the array $[S^{B,F}(x)]$ given in Eq. (75).

Similarly, replacing $F(\mathbf{x})$ in Eq. (78) with $T^{LF}_{\beta\kappa\gamma\theta\chi}(\mathbf{x})$ given in Eqs. (76) and (77) yields, with the help of Eqs. (80c-e),

$$\langle T^{LF}_{\beta\kappa\gamma\theta\chi}(\mathbf{x}) \rangle_A = 0. \quad (85)$$

That is, the average of $T^{LF}_{\beta\kappa\gamma\theta\chi}(\mathbf{x})$ over the cylindrical inclusion vanishes.

It then follows from Eqs. (31), (78) and (85) that

$$\langle \varepsilon_{\alpha\beta} \rangle_A = \langle S^{LF}_{\alpha\beta\gamma\theta} \rangle_A \varepsilon_{\gamma\theta}^*, \quad (86)$$

where $\langle S^{LF}_{\alpha\beta\gamma\theta} \rangle_A$ is given in Eqs. (81)–(84a-c). Eq. (86) shows that the average disturbed strain is only related to the eigenstrain ε^* even in the presence of the eigenstrain gradient κ^* . This result is very important for homogenization analyses of heterogeneous materials based on higher-order elasticity theories (e.g., Ma and Gao, 2010b).

4. Numerical results

Several numerical examples are presented in this section to quantitatively illustrate how the components of the Eshelby tensor for the finite-domain cylindrical inclusion problem derived in Section 3 change with the position \mathbf{x} , inclusion size a and matrix size H . For illustration purposes, in the numerical analyses provided here the Poisson's ratio ν is taken to be 0.3, and the material length scale parameter L to be 17.6 μm , as was done in earlier studies (e.g., Gao and Ma, 2010a; Ma and Gao, 2010a).

Fig. 5 shows the distribution of $S^{LF}_{1111} (= S^{L,C}_{1111} + S^{L,G}_{1111} + S^{B,F}_{1111})$ along the x_1 axis (or any radial direction due to the axisymmetry) of a cylindrical inclusion concentrically embedded in a finite cylindrical elastic matrix. The values of S^{LF}_{1111} displayed in Fig. 5 are obtained from Eqs. (74), (75), (39a), (39c), (39d) and (40a-f) and normalized by $S^{L,C}_{1111}$, which is a constant (i.e., $S^{L,C}_{1111} = 0.6786$ from Eqs. (38) and (39a-c)). The inclusion has a fixed size of $a = L$, while the matrix has four different sizes: $H = 2a$, $H = 3a$, $H = 5a$, and $H = 10a$, as indicated in Fig. 5. For comparison, the distribution of $S^{L,\infty}_{1111} (= S^{L,C}_{1111} + S^{L,G}_{1111})$ for the unbounded cylindrical inclusion problem (with $H \rightarrow \infty$) along the same direction is also plotted. The value of $S^{L,\infty}_{1111}$ is determined from Eqs. (38)–(40a-f) and incorporates the gradient effect but not the boundary effect.

As displayed in Fig. 5, the values of S^{LF}_{1111} for the bounded-domain inclusion problem are larger than those of $S^{L,\infty}_{1111}$ for the unbounded-domain inclusion problem in all cases considered. The distance between the curves for S^{LF}_{1111} and that for $S^{L,\infty}_{1111}$ decreases as H increases from $2a$ to $10a$ or as the inclusion volume fraction, ϕ , defined by $\phi = (a/H)^2$, decreases from 25% to 1%. The decreasing distance indicates that the contribution of the boundary part $S^{B,F}_{1111} (= S^{LF}_{1111} - S^{L,\infty}_{1111})$ decreases with decreasing ϕ . When $H = 10a$,

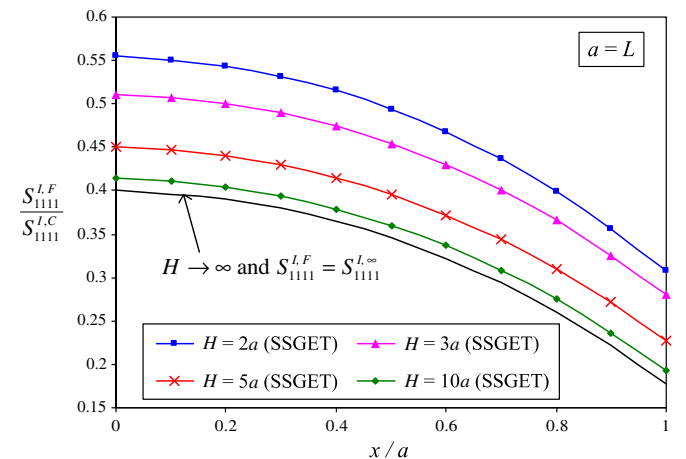


Fig. 5. S^{LF}_{1111} along a radial direction of the inclusion for the matrix with different sizes.

ϕ is very small (with $\phi = 1\%$), and $S_{1111}^{I,F}$ is quite close to $S_{1111}^{I,\infty}$, implying that the contribution of the boundary part is insignificant and may therefore be ignored. However, the contribution of $S_{1111}^{B,F}$ to the total value of $S_{1111}^{I,F}$ increases with increasing ϕ . As ϕ increases to 25% (i.e., H decreases to $2a$), $S_{1111}^{I,F}$ becomes much larger than $S_{1111}^{I,\infty}$, indicating that the boundary effect is significant and can no longer be neglected. Clearly, Fig. 5 shows that the value of $S_{1111}^{I,\infty}$ (a component of the Eshelby tensor with no boundary effect) provides a lower bound of the values of $S_{1111}^{I,F}$ (the counterpart component of the Eshelby tensor including the boundary effect).

The variation of the component of the averaged Eshelby tensor inside the inclusion is illustrated in Fig. 6. The distributions of $\langle S_{1111}^{I,F} \rangle_A (= \langle S_{1111}^{I,\infty} \rangle_A + \langle S_{1111}^{B,F} \rangle_A)$ for the finite-domain cylindrical inclusion problem based on the SSGET are shown as solid curved lines with markers, while those of $\langle S_{1111}^{I,F} \rangle_A$ based on classical elasticity are displayed as dashed straight lines. The values of $\langle S_{1111}^{I,\infty} \rangle_A$ for the unbounded-domain cylindrical inclusion problem (i.e., $\phi \rightarrow 0$) based on the SSGET/classical elasticity are also plotted in Fig. 6 for comparison. Note that the values of $\langle S_{1111}^{I,F} \rangle_A$ shown in Fig. 6 are obtained from Eqs. (81)–(84a–c), with those for the classical elasticity-based cases determined by setting $L \rightarrow 0$. From Eq. (82) it is seen that $\langle S_{1111}^{I,\infty} \rangle_A$ based on the SSGET is independent of H and is therefore the same for all of the SSGET-based $\langle S_{1111}^{I,F} \rangle_A$ curves with different values of ϕ shown in Fig. 6 (including the curve with $\phi \rightarrow 0$ or $H \rightarrow \infty$). Therefore, the distance between a line for $\langle S_{1111}^{I,F} \rangle_A$ with a specified $\phi (\neq 0)$ and the line for $\langle S_{1111}^{I,\infty} \rangle_A$ with $\phi \rightarrow 0$, based on either the SSGET or classical elasticity, are actually the boundary part $\langle S_{1111}^{B,F} \rangle_A (= \langle S_{1111}^{I,F} \rangle_A - \langle S_{1111}^{I,\infty} \rangle_A)$ (see Eq. (81)).

Fig. 6 displays the inclusion size effect predicted by the solutions based on the SSGET for both the current finite-domain inclusion problem (with different values of $\phi \neq 0$) and the unbounded-domain problem (with $\phi \rightarrow 0$). That is, in each case with a fixed inclusion volume fraction ϕ , the smaller the inclusion radius a is, the smaller the value of $\langle S_{1111}^{I,F} \rangle_A$ is. This size effect is seen to be more significant for the cases with small inclusion volume fractions, where the boundary effect is small, as will be discussed below. However, as the inclusion size becomes large (with

$a > 264 \mu\text{m}$ or $a/L > 15$ for $\phi = 16\%$ here), the size effect is seen to be diminishing. In contrast, the solution based on classical elasticity gives a constant value of $\langle S_{1111}^{I,F} \rangle_A$ for each value of ϕ , which provides an upper bound of the values of $\langle S_{1111}^{I,F} \rangle_A$ based on the SSGET for the same value of ϕ , as shown in Fig. 6. Nevertheless, each of these constant values is independent of the inclusion radius a , indicating that the classical elasticity-based solution for the finite-domain inclusion problem does not have the capability to predict the inclusion size effect.

From Fig. 6 it is also observed that $\langle S_{1111}^{I,F} \rangle_A$ changes with the inclusion volume fraction ϕ : the smaller ϕ is, the smaller $\langle S_{1111}^{I,F} \rangle_A$ is, and the closer the curve of $\langle S_{1111}^{I,F} \rangle_A$ is to that of $\langle S_{1111}^{I,\infty} \rangle_A$ (with $\phi \rightarrow 0$). This indicates that the boundary effect, as measured by $\langle S_{1111}^{B,F} \rangle_A (= \langle S_{1111}^{I,F} \rangle_A - \langle S_{1111}^{I,\infty} \rangle_A)$, becomes smaller as ϕ gets smaller. However, when ϕ is big enough (with $\phi = 16\%$ and above here), $\langle S_{1111}^{B,F} \rangle_A$ and therefore the boundary effect become significantly large. The same is true for all of the other non-vanishing components of $\langle S_{1111}^{I,F} \rangle_A$, which is dictated by Eqs. (83) and (84a–c). These observations indicate that the boundary effect is insignificant and may be neglected only when the inclusion volume fraction is sufficiently low. In addition, the numerical results reveal that the average Eshelby tensor for the finite-domain cylindrical inclusion problem is bounded from below by the average Eshelby tensor based on the SSGET for the infinite-domain cylindrical inclusion problem and is bounded from above by the average Eshelby tensor based on classical elasticity for the same inclusion problem.

5. Summary and concluding remarks

An Eshelby-type inclusion problem of a finite plane strain elastic body of arbitrary cross-sectional shape containing an arbitrarily-shaped inclusion prescribed with a uniform eigenstrain and a uniform eigenstrain gradient is solved using a simplified strain gradient elasticity theory (SSGET). An extended Betti's reciprocal theorem and an extended Somigliana's identity based on the SSGET and suitable for plane strain problems are employed in the formulation. The displacement field induced by the eigenstrain and eigenstrain gradient is expressed as a general integral representation in terms of the SSGET-based Green's function for an infinite plane strain elastic body. It contains an area integral and a line integral, the former of which is the same as that for the plane strain inclusion problem with an infinite matrix and the latter of which represents the boundary effect. This solution recovers that for the unbounded-domain plane strain inclusion problem based on the SSGET derived in Ma and Gao (2010a) if the boundary effect is suppressed.

The Eshelby tensor for the finite-domain inclusion problem of a cylindrical inclusion embedded concentrically in a finite cylindrical matrix of an enhanced continuum obeying the SSGET is derived in a closed form for the first time by using the general solution. Its average over the circular cross-sectional area of the inclusion is also obtained analytically. Being dependent on the position, inclusion size, matrix size, and material length scale parameter, this Eshelby tensor can capture both the inclusion size and the boundary effects, unlike existing ones for bounded- or unbounded-domain inclusion problems. In the absence of both the strain gradient and boundary effects, the newly obtained Eshelby tensor recovers that for the unbounded-domain plane strain cylindrical inclusion problem based on classical elasticity.

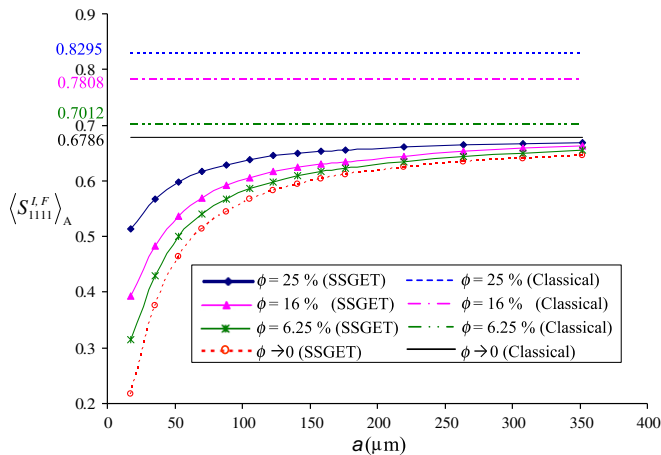


Fig. 6. $\langle S_{1111}^{I,F} \rangle_A$ varying with the inclusion size at different inclusion volume fractions.

Numerical examples are provided to quantitatively illustrate the newly obtained Eshelby tensor for the finite-domain cylindrical inclusion problem. The results show that the inclusion size effect can be significant if the inclusion is small and that the boundary effect can be dominant if the inclusion volume fraction is large. But the inclusion size effect becomes insignificant when the inclusion gets large, and the boundary effect tends to be negligibly small at a sufficiently low inclusion volume fraction. In addition, it is found that the components of both the Eshelby tensor and its average for the finite-domain cylindrical inclusion problem are bounded from below by their counterparts for the infinite-domain cylindrical inclusion problem based on the SSGT. Furthermore, the averaged Eshelby tensor for the finite-domain cylindrical inclusion problem based on the SSGT is bounded from above by its counterpart based on classical elasticity.

Finally, it should be mentioned that the general approach based on the Green's function method and extended Betti's reciprocal theorem and Somigliana's identity presented in this paper can also be used to solve finite-domain anti-plane strain inclusion problems, which are closely related to the cylindrical inclusion problem studied here. Anti-plane strain inclusion problems are simpler than plane strain and other 2-D and 3-D inclusion problems and have been extensively studied (e.g., Pak, 1992; Gao, 1996; Gao and Li, 2005; Lubarda, 2003; Le Quang et al., 2008; Haftbaradaran and Shodja, 2009). In particular, it was shown in Le Quang et al. (2008) that within the context of classical elasticity the Eshelby tensor for the infinite-domain anti-plane strain inclusion problem is a second-order tensor (rather than a fourth-order tensor as in plane strain and other 2-D and 3-D inclusion problems). Also, it was found in Lubarda (2003) that the Eshelby tensor based on a couple stress elasticity theory is non-uniform inside an inclusion prescribed with a uniform eigenstrain of anti-plane shear type. These two Eshelby tensors were both obtained for problems with unbounded elastic matrices. Therefore, there is still a need to study finite-domain anti-plane strain inclusion problems using higher-order elasticity theories such as the SSGT. In response to this need, such a study has been undertaken and will be reported separately.

Acknowledgements

The work reported in this paper is supported by a grant from the U.S. National Science Foundation, with Dr. Clark V. Cooper as the program manager. This support is gratefully acknowledged. The authors also thank Professor David A. Hills and two anonymous reviewers for their encouragement and helpful comments on an earlier version of the paper.

Appendix A

In this appendix, the expressions of the transformation tensors $T_{\alpha\beta}(\mathbf{y} - \mathbf{x})$ and $Q_{\alpha\beta}(\mathbf{y} - \mathbf{x})$ given in Eqs. (17a,b) are derived.

From Eqs. (2a) and (3), it follows that

$$\tau_{\alpha\beta} = \lambda u_{\gamma,\gamma} \delta_{\alpha\beta} + \mu(u_{\alpha,\beta} + u_{\beta,\alpha}). \quad (A1)$$

Using Eq. (15) in Eq. (A1) gives

$$\tau_{\alpha\beta} = P_{\alpha\beta\gamma} e_{\gamma} \quad (A2)$$

with

$$P_{\alpha\beta\gamma} \equiv \lambda G_{0\gamma,0} \delta_{\alpha\beta} + \mu(G_{\alpha\gamma,\beta} + G_{\beta\gamma,\alpha}). \quad (A3)$$

Substituting Eqs. (4) and (6) into Eq. (8c) results in

$$t_{\alpha} = \tau_{\alpha\beta} n_{\beta} + L^2 \left[-(\nabla^2 \tau_{\alpha\beta}) n_{\beta} - \tau_{\alpha\beta,0} n_0 + \tau_{\alpha\beta,\chi} n_{\chi} n_{\beta} \right] + L^2 \tau_{\alpha\beta,0} (-n_{0,\beta} + n_{0,\chi} n_{\chi} n_{\beta} + n_0 n_{\chi,\chi} n_{\beta}). \quad (A4)$$

Using Eq. (A2) in (A4) yields

$$t_{\alpha} = T_{\alpha\gamma} e_{\gamma}, \quad (A5)$$

where

$$T_{\alpha\gamma} = P_{\alpha\beta\gamma} n_{\beta} - L^2 (\nabla^2 P_{\alpha\beta\gamma}) n_{\beta} - L^2 P_{\alpha\beta\gamma,0} n_0 + L^2 P_{\alpha\beta\gamma,\chi} n_{\chi} n_{\beta} + L^2 P_{\alpha\beta\gamma,0} (-n_{0,\beta} + n_{0,\chi} n_{\chi} n_{\beta} + n_0 n_{\chi,\chi} n_{\beta}). \quad (A6)$$

The expression of the Cauchy traction transformation tensor $T_{\alpha\gamma}$ obtained in Eq. (A6) is exactly what is given in Eq. (17a).

Next, using Eqs. (4) and (A2) in Eq. (8d) leads to

$$q_{\alpha} = Q_{\alpha\gamma} e_{\gamma}, \quad (A7)$$

where

$$Q_{\alpha\gamma} = L^2 P_{\alpha\beta\gamma,\chi} n_{\beta} n_{\chi}. \quad (A8)$$

The expression of the double stress traction transformation tensor $Q_{\alpha\gamma}$ given in Eq. (A8) is the same as that listed in Eq. (17b). This completes the derivation of Eqs. (17a) and (17b).

Appendix B

In this appendix, the integral results given in Eqs. (55) and (56) are proved.

To evaluate the line integrals along the circle ∂R with radius H in Eqs. (55) and (56), a particular 2-D Cartesian coordinate system is chosen such that the \mathbf{e}_1 axis is along the direction of position vector \mathbf{x} (with $0 < |\mathbf{x}| < H$), as shown in Fig. 4. In such a coordinate system, the unit vector \mathbf{n} , which represents the direction of position vector \mathbf{y} (with $|\mathbf{y}| = H$) and coincides with the outward unit normal vector on ∂R can be expressed as

$$\mathbf{n} = \cos \theta \mathbf{e}_1 + \sin \theta \mathbf{e}_2, \quad (B1)$$

where $\theta \in [0, \pi]$ is the angle between \mathbf{x} and \mathbf{y} . Also, the distance between \mathbf{x} and \mathbf{y} , r , can be obtained from the cosine law as

$$r = |\mathbf{x} - \mathbf{y}| = \sqrt{x^2 + H^2 - 2xH \cos \theta}, \quad (B2)$$

where $x = |\mathbf{x}|$ and $H = |\mathbf{y}|$.

Note that the 2-D Cartesian coordinate system represented by the base vectors \mathbf{e}_1 and \mathbf{e}_2 can be rotated into a new system with base vectors $\hat{\mathbf{e}}_1$ and $\hat{\mathbf{e}}_2$ (see Fig. 4). In terms of $\hat{\mathbf{e}}_1$ and $\hat{\mathbf{e}}_2$ the unit vector \mathbf{n} can be written as

$$\mathbf{n} = \cos \theta R_{1\alpha} \hat{\mathbf{e}}_{\alpha} + \sin \theta R_{2\alpha} \hat{\mathbf{e}}_{\alpha}, \quad (B3)$$

or, in the index form,

$$n_{\alpha} = \cos \theta R_{1\alpha} + \sin \theta R_{2\alpha}, \quad (B4)$$

where $R_{\alpha\beta}$ are the components of the rotation tensor satisfying $\mathbf{e}_{\alpha} = R_{\alpha\beta} \hat{\mathbf{e}}_{\beta}$ and

$$R_{\gamma\alpha} R_{\gamma\beta} = R_{1\alpha} R_{1\beta} + R_{2\alpha} R_{2\beta} = \delta_{\alpha\beta}. \quad (B5)$$

The line integral of $f(r)n_{\alpha}$ along ∂R is given by

$$\langle f(r)n_{\alpha} \rangle \equiv \int_{\partial R} f(r)n_{\alpha} dS_{\gamma} = H \int_0^{2\pi} f(r)n_{\alpha} d\theta, \quad (B6)$$

where use has been made of the line element $dS_{\gamma} = H d\theta$ on the circle ∂R . Using Eqs. (B2) and (B4) and the fact that the position vector \mathbf{x} coincides with the \mathbf{e}_1 axis (i.e., $\mathbf{x}^0 = \mathbf{e}_1 = R_{1\alpha} \hat{\mathbf{e}}_{\alpha}$ or $x_{\alpha}^0 = R_{1\alpha}$), Eq. (B6) can be rewritten as

$$\langle f(r)n_{\alpha} \rangle = \left[\frac{H}{x} \int_0^{2\pi} f(r) \cos \theta d\theta \right] x_{\alpha}, \quad (B7)$$

where $x_{\alpha} = x x_{\alpha}^0$. Eq. (B7) is exactly what is given in Eqs. (55) and (57a).

Next, note that with the help of Eq. (B3) the integral of $f(r)n_\alpha n_\beta$ along the circle ∂R becomes

$$\begin{aligned} \langle f(r)n_\alpha n_\beta \rangle &\equiv \int_{\partial R} f(r)n_\alpha n_\beta dS_\gamma = H \int_0^{2\pi} f(r)n_\alpha n_\beta n_\gamma d\theta \\ &= H \int_0^{2\pi} f(r)[\cos^3 \theta R_{1\alpha} R_{1\beta} R_{1\gamma} + \sin^3 \theta R_{2\alpha} R_{2\beta} R_{2\gamma} \\ &\quad + \sin^2 \theta \cos \theta (R_{2\alpha} R_{2\beta} R_{1\gamma} + R_{2\alpha} R_{1\beta} R_{2\gamma} + R_{1\alpha} R_{2\beta} R_{2\gamma}) \\ &\quad + \sin \theta \cos^2 \theta (R_{1\alpha} R_{2\beta} R_{1\gamma} + R_{2\alpha} R_{1\beta} R_{1\gamma} \\ &\quad + R_{1\alpha} R_{1\beta} R_{2\gamma})] d\theta. \end{aligned} \quad (\text{B8})$$

It can be readily shown that

$$\int_0^{2\pi} f(r) \sin^3 \theta d\theta = 0, \quad \int_0^{2\pi} f(r) \sin \theta \cos^2 \theta d\theta = 0, \quad (\text{B9})$$

where r is defined in Eq. (B2).

Using Eqs. (B9) and (B5) and $x_\alpha^0 = R_{1\alpha}$ in Eq. (B8) leads to

$$\begin{aligned} \langle f(r)n_\alpha n_\beta \rangle &= \left[\frac{H}{x^3} \int_0^{2\pi} f(r)(4\cos^3 \theta - 3\cos \theta) d\theta \right] x_\alpha x_\beta x_\gamma \\ &\quad + \left[\frac{H}{x} \int_0^{2\pi} f(r)(\cos \theta - \cos^3 \theta) d\theta \right] (\delta_{\alpha\beta} x_\gamma + \delta_{\alpha\gamma} x_\beta + \delta_{\beta\gamma} x_\alpha). \end{aligned} \quad (\text{B10})$$

Eq. (B10) is the same as that listed in Eqs. (56) and (57b,c).

References

- Arfken, G.B., Weber, H.-J., 2005. *Mathematical Methods for Physicists*, sixth ed. Elsevier, San Diego.
- Budiansky, B., 1965. On the elastic moduli of some heterogeneous materials. *J. Mech. Phys. Solids* 13, 223–227.
- Cheng, Z.-Q., He, L.-H., 1995. Micropolar elastic fields due to a spherical inclusion. *Int. J. Eng. Sci.* 33, 389–397.
- Cheng, Z.-Q., He, L.-H., 1997. Micropolar elastic fields due to a circular cylindrical inclusion. *Int. J. Eng. Sci.* 35, 659–668.
- Cho, J., Joshi, M.S., Sun, C.T., 2006. Effect of inclusion size on mechanical properties of polymeric composites with micro and nano particles. *Compos. Sci. Technol.* 66, 1941–1952.
- Eshelby, J.D., 1957. The determination of the elastic field of an ellipsoidal inclusion, and related problems. *Proc. R. Soc. Lond. A* 241, 376–396.
- Eshelby, J.D., 1959. The elastic field outside an ellipsoidal inclusion. *Proc. R. Soc. Lond. A* 252, 561–569.
- Gao, X.-L., 1996. A mathematical analysis of the elasto-plastic anti-plane shear problem of a power-law material and one class of closed-form solutions. *Int. J. Solids Struct.* 33, 2213–2223.
- Gao, X.-L., Li, K., 2005. A shear-lag model for carbon nanotube-reinforced polymer composites. *Int. J. Solids Struct.* 42, 1649–1667.
- Gao, X.-L., Ma, H.M., 2009. Green's function and Eshelby's tensor based on a simplified strain gradient elasticity theory. *Acta Mech.* 207, 163–181.
- Gao, X.-L., Ma, H.M., 2010a. Solution of Eshelby's inclusion problem with a bounded domain and Eshelby's tensor for a spherical inclusion in a finite spherical matrix based on a simplified strain gradient elasticity theory. *J. Mech. Phys. Solids* 58, 779–797.
- Gao, X.-L., Ma, H.M., 2010b. Strain gradient solution for Eshelby's ellipsoidal inclusion problem. *Proc. R. Soc. A* 466, 2425–2446.
- Gao, X.-L., Park, S.K., 2007. Variational formulation of a simplified strain gradient elasticity theory and its application to a pressurized thick-walled cylinder problem. *Int. J. Solids Struct.* 44, 7486–7499.
- Gao, X.-L., Rowlands, R.E., 2000. Hybrid method for stress analysis of finite three-dimensional elastic components. *Int. J. Solids Struct.* 37, 2727–2751.
- Genin, G.M., Birman, V., 2009. Micromechanics and structural response of functionally graded, particulate-matrix, fiber-reinforced composites. *Int. J. Solids Struct.* 46, 2136–2150.
- Gradshteyn, I.S., Ryzhik, I.M., 2007. *Table of Integrals, Series, and Products*, seventh ed. Academic Press, Boston.
- Haftbaradaran, H., Shodja, H.M., 2009. Elliptic inhomogeneities and inclusions in anti-plane couple stress elasticity with application to nano-composites. *Int. J. Solids Struct.* 46, 2978–2987.
- Hill, R., 1965. A self-consistent mechanics of composites materials. *J. Mech. Phys. Solids* 13, 213–222.
- Huang, Y., Hu, K.X., Wei, X., Chandra, A., 1994. A generalized self-consistent mechanics method for composite materials with multiphase inclusions. *J. Mech. Phys. Solids* 42, 491–504.
- Kinoshita, N., Mura, T., 1984. Eigenstrain problems in a finite elastic body. *SIAM J. Appl. Math.* 44, 524–535.
- Kiris, A., Inan, E., 2006. Eshelby tensors for a spherical inclusion in microstretch elastic fields. *Int. J. Solids Struct.* 43, 4720–4738.
- Le Quang, H., He, Q.-C., 2007. A one-parameter generalized self-consistent model for isotropic multiphase composites. *Int. J. Solids Struct.* 44, 6805–6825.
- Le Quang, H., He, Q.-C., Zheng, Q.-S., 2008. Some general properties of Eshelby's tensor fields in transport phenomena and anti-plane elasticity. *Int. J. Solids Struct.* 45, 3845–3857.
- Li, S., Sauer, R.A., Wang, G., 2005. A circular inclusion in a finite domain I. The Dirichlet-Eshelby problem. *Acta Mech.* 179, 67–90.
- Li, S., Sauer, R.A., Wang, G., 2007. The Eshelby tensors in a finite spherical domain – Part I: Theoretical formulations. *ASME J. Appl. Mech.* 74, 770–783.
- Li, S., Wang, G., 2008. *Introduction to Micromechanics and Nanomechanics*. World Scientific, Singapore.
- Liu, X.N., Hu, G.K., 2004. Inclusion problem of microstretch continuum. *Int. J. Eng. Sci.* 42, 849–860.
- Lubarda, V.A., 2003. Circular inclusions in anti-plane strain couple stress elasticity. *Int. J. Solids Struct.* 40, 3827–3851.
- Ma, H.M., Gao, X.-L., 2010a. Eshelby's tensors for plane strain and cylindrical inclusions based on a simplified strain gradient elasticity theory. *Acta Mech.* 211, 115–129.
- Ma, H.M., Gao, X.-L., 2010b. A homogenization method for multiphase composites using strain gradient elasticity-based Eshelby tensors. (manuscript to be published).
- Ma, H.S., Hu, G.K., 2006. Eshelby tensors for an ellipsoidal inclusion in a micropolar material. *Int. J. Eng. Sci.* 44, 595–605.
- Ma, H.S., Hu, G.K., 2007. Eshelby tensors for an ellipsoidal inclusion in a microstretch material. *Int. J. Solids Struct.* 44, 3049–3061.
- Magnus, W., Oberhettinger, F., Soni, R.P., 1966. *Formulas and Theorems for the Special Functions of Mathematical Physics*. Springer-Verlag, New York.
- Mindlin, R.D., 1964. Micro-structure in linear elasticity. *Arch. Ration. Mech. Anal.* 16, 51–78.
- Mindlin, R.D., 1965. Second gradient of strain and surface-tension in linear elasticity. *Int. J. Solids Struct.* 1, 417–438.
- Mindlin, R.D., Eshel, N.N., 1968. On first strain-gradient theories in linear elasticity. *Int. J. Solids Struct.* 4, 109–124.
- Mori, T., Tanaka, K., 1973. Average stress in matrix and average elastic energy of materials with misfitting inclusions. *Acta Metall.* 21, 571–574.
- Pak, Y.E., 1992. Circular inclusion problem in antiplane piezoelectricity. *Int. J. Solids Struct.* 29, 2403–2419.
- Paris, F., Canas, J., 1997. *Boundary Element Method: Fundamentals and Applications*. Oxford Science Publications, Oxford.
- Polyzos, D., Tsepoura, K.G., Tsinopoulos, S.V., Beskos, D.E., 2003. A boundary element method for solving 2-D and 3-D static gradient elastic problems: Part I: Integral formulation. *Comput. Methods Appl. Mech. Eng.* 192, 2845–2873.
- Qu, J., Cherkouhi, M., 2006. *Fundamentals of Micromechanics of Solids*. Wiley, Hoboken, NJ.
- Reynaud, E., Jouen, T., Gauthier, C., Vigier, G., Varlet, J., 2001. Nanofillers in polymeric matrix: a study on silica reinforced PA6. *Polymer* 42, 8759–8768.
- Timoshenko, S.P., Goodier, J.N., 1970. *Theory of Elasticity*, third ed. McGraw-Hill, New York.
- Vollenberg, P.H.T., Heikens, D., 1989. Particle size dependence of the Young's modulus of filled polymers: 1. Preliminary experiments. *Polymer* 30, 1656–1662.
- Weng, G.J., 1990. The theoretical connection between Mori-Tanaka's theory and the Hashin-Shtrikman-Walpole bounds. *Int. J. Eng. Sci.* 28, 1111–1120.
- Zhang, X., Sharma, P., 2005. Inclusions and inhomogeneities in strain gradient elasticity with couple stresses and related problems. *Int. J. Solids Struct.* 42, 3833–3851.
- Zheng, Q.-S., Zhao, Z.-H., 2004. Green's function and Eshelby's fields in couple-stress elasticity. *Int. J. Multiscale Comput. Eng.* 2, 15–27.